Copyright Warning & Restrictions

The copyright law of the United States (Title 17, United States Code) governs the making of photocopies or other reproductions of copyrighted material.

Under certain conditions specified in the law, libraries and archives are authorized to furnish a photocopy or other reproduction. One of these specified conditions is that the photocopy or reproduction is not to be "used for any purpose other than private study, scholarship, or research." If a, user makes a request for, or later uses, a photocopy or reproduction for purposes in excess of "fair use" that user may be liable for copyright infringement,

This institution reserves the right to refuse to accept a copying order if, in its judgment, fulfillment of the order would involve violation of copyright law.

Please Note: The author retains the copyright while the New Jersey Institute of Technology reserves the right to distribute this thesis or dissertation

Printing note: If you do not wish to print this page, then select "Pages from: first page # to: last page #" on the print dialog screen

ABSTRACT

ON GREENING OPTICAL ACCESS NETWORKS

by
Mina Taheri Hosseinabadi

With the remarkable growth of fiber-based services, the number of FTTx subscribers has been dramatically increasing in recent years. Owing to the environmental concern, reducing energy consumption of optical access networks has become an important issue for network designers. In Ethernet passive optical network (EPON), the optical line terminal (OLT) located at the central office broadcasts the downstream traffic to all optical network units (ONUs), each of which checks all arrival downstream packets to obtain those destined to itself. Since traffic of ONUs changes dynamically, properly defining the sleep mode for idle ONUs can potentially save a significant amount of energy. However, it is challenging to shut down an ONU receiver as the ONU needs to receive some downstream control packets to perform upstream transmission. In this framework, a novel sleep control scheme is proposed to address the downstream issue which can efficiently put ONU receivers to sleep. This dissertation further defines multiple levels of power saving in which the ONU disables certain functions based on the upstream and downstream traffic load. The proposed schemes are completely compatible with the multi-point control protocol (MPCP) and EPON standards. Elimination of the handshake process makes the sleep control schemes more efficient. Currently, OLTs also consume a significant amount of energy in EPON. Therefore, reducing energy consumption of OLT is as important as reducing energy consumption of ONUs; such requirement becomes even more urgent as OLT keeps increasing its provisioning data rate, and higher data rate provisioning usually implies higher energy consumption. Thus, a novel energy-efficient OLT structure, which guarantees services of end users with a smallest number of power-on OLT line cards, is proposed. More specifically, the number of power-on OLT line cards is adapted to the real-time incoming traffic. Also, to avoid service disruption resulted by powering off OLT line cards, a proper optical switch is equipped in OLT to dynamically configure the communications between OLT line cards and ONUs. By deploying a semi-Markov based technique, the performance characteristics of the sleep control scheme such as delay and

energy-saving are theoretically analyzed. It is shown that, with proper settings of sleep control parameters, the proposed scheme can save a significant amount of energy in EPON.

ON GREENING OPTICAL ACCESS NETWORKS

by
Mina Taheri Hosseinabadi

A Dissertation
Submitted to the Faculty of
New Jersey Institute of Technology
in Partial Fulfillment of the Requirements for the Degree of
Doctor of Philosophy in Electrical Engineering

Helen and John C. Hartmann Department of
Electrical and Computer Engineering

May 2016

APPROVAL PAGE

ON GREENING OPTICAL ACCESS NETWORKS

Mina Taheri Hosseinabadi

Dr. Nirwan Ansari, Dissertation Advisor — Date
Distinguished Professor of Electrical and Computer Engineering, NJIT

Dr. Ahmad Khalil, Committee Member — Date
Network Architect, TATA Communications

Dr. Abdallah Khreishah, Committee Member — Date
Assistant Professor of Electrical and Computer Engineering, NJIT

Dr. Roberto Rojas-Cessa, Committee Member — Date
Associate Professor of Electrical and Computer Engineering, NJIT

Dr. Mengchu Zhou, Committee Member — Date
Distinguished Professor of Electrical and Computer Engineering, NJIT

BIOGRAPHICAL SKETCH

Author: Mina Taheri Hosseinabadi

Degree: Doctor of Philosophy

Date: May 2016

Undergraduate and Graduate Education:

- Doctor of Philosophy in Electrical Engineering, 2016
  New Jersey Institute of Technology, Newark, NJ
- Master of Science in Electrical Engineering,
  Isfahan University of Technology, Isfahan, Iran, 2010
- Bachelor of Science in Electrical Engineering,
  Isfahan University of Technology, Isfahan, Iran, 2004

Major: Electrical Engineering

Presentations and Publications:

M. Taheri and N. Ansari, "A Feasible Solution to Provide Cloud Computing over Optical Networks," *IEEE Network*, vol. 27, no. 6, pp. 31-35, 2013.

M. Taheri and N. Ansari, "Chapter 2: FiWi Networks," *Intelligent Systems for Optical Networks Design: Advancing Techniques* (Y. S. Kavian and Z. Ghassemlooy, eds.), Hershey, PA: IGI Global, ISBN13: 9781466636521, 2013.

J. Zhang, M. Taheri, and N. Ansari, "Standards-compliant EPON Sleep Control for Energy Efficiency: Design and Analysis," *IEEE/OSA Journal of Optical Communications and Networking*, vol. 5, no. 7, pp. 677-685, 2013.

M. Taheri and N. Ansari, "Multi-power-level Energy Saving Management for Passive Optical Networks," *IEEE/OSA Journal of Optical Communications and Networking*, vol. 6, no. 11, pp. 965-973, 2014.

M. Taheri and N. Ansari, "Power-aware Admission Control and Virtual Machine Allocation for Cloud Applications," *36th IEEE Sarnoff Symposium*, Newark, NJ, pp. 134-139, Sep. 20-22, 2015.

M. Taheri, J. Zhang and N. Ansari, "Design and Analysis of Green Optical Line Terminal for TDM Passive Optical Networks," *IEEE/OSA Journal of Optical Communications and Networking*, vol. 8, no. 4, pp. 221-228, April 2016.

N. Ansari, T. Han, and M. Taheri "GATE: Greening At The Edge," *IEEE Wireless Communications*, to appear in April 2016.

M. Taheri, N. Ansari, J. Feng, R. Rojas-Cessa, and M. Zhou, "FOCUS: Free space OptiCs Utilization in high-Speed trains," *IEEE Vehicular Technology Magazine*, submitted, 2016.

Dedicated to my husband and my parents.

ACKNOWLEDGMENT

I would like to express my heartfelt gratitude and deepest appreciation to my adviser Dr. Nirwan Ansari for his wisdom, commitment, guidance and inspiration toward my research. His constructive criticism and trusting support made this work a great learning experience.

I would like to express my sincere gratitude to Dr. Ahmad Khalil, Dr. Abdallah Khreishah, Dr. Roberto Rojas-Cessa, and Dr. Mengchu Zhou for serving as committee members. I appreciate their time as well as their encouraging and constructive comments, feedback and guidance on the dissertation.

It is my honor to thank my family for being supportive and encouraging. Specifically, I would like to thank my husband, Behzad, who has been with me, side by side and through all ups and downs. Without him, I could not have achieved any of the serious goals.

TABLE OF CONTENTS

Chapter **Page**

TABLE OF CONTENTS
(Continued)

Chapter **Page**

LIST OF FIGURES

LIST OF FIGURES
(Continued)

Figure **Page**

CHAPTER 1

OVERVIEW AND MOTIVATION

Wireline broadband access networks usually deliver higher data rates than wireless access networks do. Since the DSL and cable technologies have some limitation in providing high bandwidth to the users, fiber technology has grabbed the attention of service providers in the recent years. The most pronouncing advantage of optical fiber is its huge bandwidth potential in comparison to other wireless and wired media. Moreover, optical networks are important due to their low complexity and power consumption.

As energy consumption is becoming an environmental and therefore social and economic issue, greening Information and Communication Technology (ICT) has attracted significant research attention recently. It was reported that Internet consumes as much as $1\% - 2.5\%$ of the total electricity in broadband enabled countries [9, 42, 19], and currently and in the medium term future, the majority of the energy of Internet is consumed by access networks owing to the large quantity of access nodes [10].

Energy consumptions of access networks depend on the access technologies. Among various access technologies including WiMAX, FTTN, and point to point optical access networks, passive optical networks (PONs) consume the smallest energy per transmission bit attributed to the proximity of optical fibers to the end users and the passive nature of the remote nodes [31]. However, as PON is deployed worldwide, it still consumes a significant amount of energy. It is desirable to reduce the energy consumption of PONs since every single watt saving will end up with overall terawatt and even larger power saving. Reducing energy consumption of PONs becomes even more important as the current PON systems evolve into next-generation PONs with increased data rate provisioning [58, 7].

1.1 Optical Access Networks

PON uses a point to multipoint network architecture which reduces the required amount of fiber and central office equipment in comparison with point to point architectures. FTTx is a generic term for any broadband network architecture using optical fiber to replace all or part of the usual metal local loop used for last mile telecommunications [21]. The generic term

was initially a generalization for several configurations of fiber deployment (FTTN, FTTC, FTTB, FTTH, etc.), all starting with FTT but differentiated by the last letter, which is substituted by an "x" in the generalization. The central goal of FTTx PLAN is to support the strategic decision process of city carriers and new local operators by performing an objective analysis that considers the varying, but always case-dependent boundary conditions where the "x" ends. The FTTx approach reduces planning uncertainties, supports a more realistic forecast of costs, and also detects potential technological dead-ends early in the design process. Specifically, operators of future FTTx networks for city environments and small regions will benefit from these flexible characteristics. To advance a positive business case, the techno-economic dependencies between the total cost of ownership and technical possibilities of the available system technologies need to be well understood. A thorough understanding of photonic technology trends and limitations matched with sophisticated optimization techniques canned in computer-based methods and tools provides a key benefit for network planners of future FTTx networks.

PON is considered an attractive solution to the first-mile problem [35]. PON minimizes the number of optical transceivers, central office terminations, and fiber deployment. The optical transmission in PON has no power requirements or active electronic parts once the signal traverses through the network. As depicted in Figure 1.1, PON consists of three main parts:

- Optical Line Terminal (OLT) resides in the Central Office (CO) and connects the PON to the metropolitan area network (MAN) or wide area network (WAN), also known as backbone or long-haul network.
- Optical Network Unit (ONU) provides the service interface to both residential and business end users.
- Optical Distributed Network (ODN) connects the OLT at the central office to the ONUs by using passive optical components, such as optical fiber, splices, and splitters [32].

There are three main types of PONs depending on the data multiplexing scheme summarized as TDM, WDM, and OFDM [44]. The currently deployed PON technology is time division multiplexing (TDM) PON, where traffic from multiple ONUs are TDM multiplexed onto the upstream wavelength. The OLT assigns a specific time slot to each ONU. Each ONU can then use the full upstream bandwidth of the optical link for the

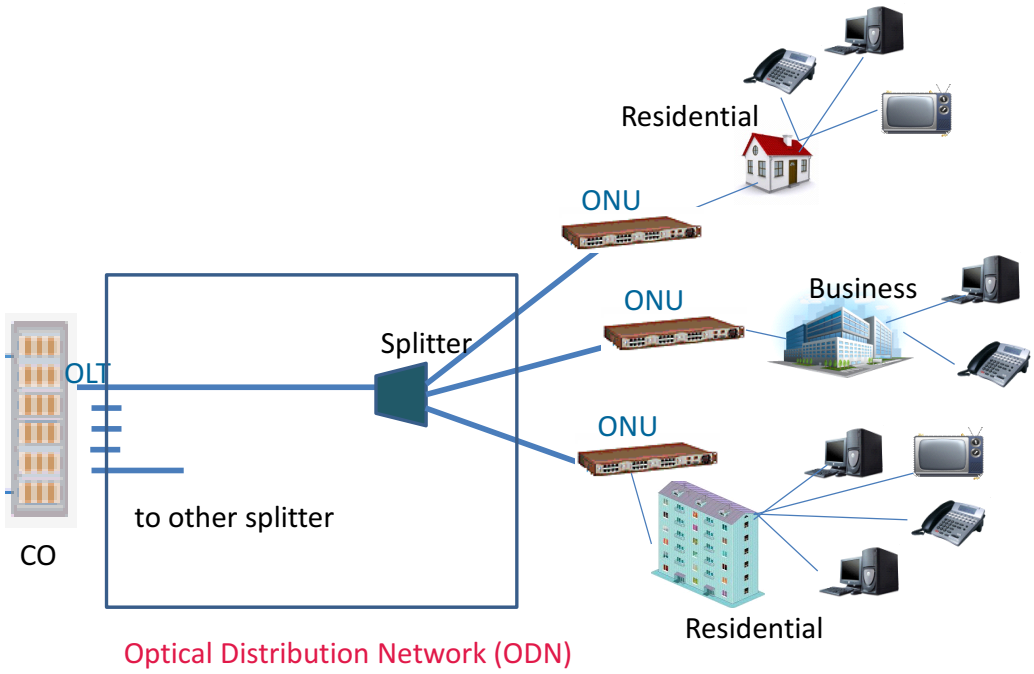

Figure 1.1 Passive Optical Network (PON).

duration of its assigned time slot. However, in the downstream direction of TDM PON, the OLT broadcasts traffic to all the connected ONUs. Wavelength division multiplexing (WDM) PON [11] uses multiple wavelengths to provision bandwidth to ONUs. Instead of the splitter used in TDM-PON architectures, WDM-PON uses an arrayed-waveguide-grating (AWG) filter that separates the wavelengths for individual delivery to the subscriber ONUs. Orthogonal frequency division multiplexing (OFDM) PON employs a number of orthogonal subcarriers to transmit traffic from/to ONUs [43]. As the WDM or OFDM technology, PONs are potentially able to provide higher than $40Gb/s$ data rate. However, the major problem for WDM PON and OFDM PON is the high deployment cost associated with these technologies.

1.2 Evolution of PON

Deployment of the fiber in the last mile in a cost-effective way is the main purpose of the current PON solutions. Two dominant PON technologies that use a TDM access mechanism are called Ethernet PON (EPON, standardized by IEEE) and Gigabit PON (GPON, standardized by ITU-T). Although there are some differences in the specifications

of these two technologies, their performance is largely determined by the underlying principle of TDM. In the following, several PON technologies advance, that have been standardized over the last decade are discussed [26, 23].

- 1G-EPON is the first generation of EPON which is spesified by IEEE 802.3ah. The standard Ethernet speed is 1 Gb/s in EPON and uses the standard 8b/10b line coding in which 8 bit data are coded to 10 line bits. Point to multipoint connectivity is supported by multipoint control protocol (MPCP) which uses standard Ethernet frames generated in the MAC layer.
- 10G-EPON was standardized by IEEE 802.3av task force that supports symmetric $10Gb/s$ downstream and upstream, and asymmetric $10Gb/s$ downstream and $1Gb/s$ upstream data rates. 10G-EPON is compatible with 1G-EPON and can coexist on the same fiber plant [46, 28].
- GPON is defined by ITU-T recommendation series G.984.1 through G.984.6. GPON also uses a generic encapsulation method to carry other protocols. It can transport Ethernet, ATM, and TDM traffic. It supports asymmetric bit rates of $2.488Gb/s$ downstream and $1.244Gb/s$ upstream.
- XG-PON architecture has been recently standardized in ITU-T (the G.987 series of Recommendations). It provides the maximum rate of $10Gb/s$ downstream and $2.5Gb/s$ upstream. Different WDM wavelengths are used, $1577nm$ downstream and $1270nm$ upstream, that allow $10Gb/s$ service to coexist on the same fiber with standard GPON.

Considering the high capacity and low-cost implementation possibilities of 10G EPON, the rest of the work focuses on different aspects of this technology.

1.3 Ethernet Passive Optical Networks

Ethernet in the First Mile is a standard ratified by IEEE to extend the existing Ethernet technology into the subscriber access area [25]. The key objective of the study was to provide a high performance network with traditional Ethernet while minimizing the deployment, maintenance and operation costs. Ethernet PON is a PON based network using Ethernet frames for encapsulating the data packets as defined in the IEEE 802.3 standard. To connect EPON to Ethernet-based networks, no conversion or encapsulation is necessary as EPON is fully compatible with the Ethernet standards. EPON is applicable to all the data-centric networks and full-service voice, data and video networks.

1.3.1 EPON Class Based Traffic

In order to support various application requirements, all the incoming traffic to each network and particularly in EPON should be segregated into a limited number of classes to provide differentiated service (Diffserv) for each class. Below are the supported traffic classifications by IEEE 802.1D [27]:

- Network control: Characterized by a "must get there" requirement to maintain and support the network infrastructure.
- Voice: Services with less than $10 - ms$ delay and maximum jitter.
- Video: Services with less than $100 - ms$ delay.
- Controlled load: Important business applications subject to some form of "admission control". That is, two extremes are to be considered; preplanning of network requirements and bandwidth reservation per flow (when flow is started).
- Excellent effort: Also known as "CEO's best effort", it refers to the best-effort-type services in which an information service association is distributed to its most important customers.
- Best effort: No QoS guarantee is made.
- Background: Bulk transfers and other activities allowed in the network should not affect the use of the network by other users and applications.

Upon receiving a packet, each ONU places it in the appropriate queue based on its classification type. EPON services are classified into three priorities: best effort (BE), assured forwarding (AF), and expedited forwarding (EF), as described in [25]. Delay sensitive services such as voice which requires bounded delay and jitter are considered as EF services. AF services require bandwidth guarantee instead of bounded delay. BE service such as Email service does not require any warranty for either bandwidth or delay.

1.3.2 EPON Scheduling

As mentioned in the previous section, different classes of services with different quality of service requirements are stored in different priority queues at each ONU. Two scheduling methods are performed to support QoS in EPON: intra-ONU scheduling and inter-ONU scheduling. The former is responsible for arbitrating the transmission of different priority queues in each ONU while the latter is responsible for arbitrating the transmission of different ONUs. Direct scheduling and hierarchical scheduling are two strategies proposed to

implement the abovementioned scheduling paradigms [62]. In direct (single level) scheduling, the scheduler located in the OLT receives information from ONUs and schedules each queue located in ONUs. Hence, the central scheduler can allocate the bandwidth fairly among the queues. Every GATE message sent to ONUs consists of several grants, each specifying the amount of time for a specific class of service allowed for a queue. Assigning a separate logical link to each queue simplifies the implementation of direct scheduling. Therefore, OLT will receive a distinct REPORT message form each unique logical link identifier (LLID), which specifies just one queue. In hierarchical (multi-level) scheduling, each ONU can execute intra-ONU scheduling while OLT executes inter-ONU scheduling. Based on the buffer occupancy, each ONU requests dedicated bandwidth from OLT. After receiving the grant from OLT, allocated bandwidth is divided among different service classes based on QoS requirements. Higher priority traffic is transmitted first in the allocated transmission window, and the remaining time is assigned to lower priority traffic. Hierarchical scheduling is scalable with the number of queues as each ONU sends one single REPORT message and receives a single GATE message to and from OLT, respectively.

1.3.3 Class Based Bandwidth Allocation in EPON

As the upstream channel of EPON is shared among end users, an efficient medium access control is required to statistically multiplex multiple services from various types of traffic. Luo and Ansari [36] provided an overview of the upstream bandwidth allocation for multiservice access over EPON. Owing to multipoint control protocol (MPCP) and bursty traffic prediction, a dynamic bandwidth allocation (DBA) scheme is also proposed to provision QoS guarantees. Multiservice access for different end users is realized by means of class-based traffic estimation. Class based bandwidth allocation is the most important factor in affecting QoS provisioning of intra ONU scheduling. OLT collects the REPORT messages from all ONUs and then decides the bandwidth allocation. Considering three aforesaid EPON classes of service, OLT first assigns fixed bandwidth to EF traffic. The remaining bandwidth is allocated to AF requests, and the unused bandwidth after serving EF and AF is then disseminated among BE requests. In strict priority scheduling, the high priority traffic arriving during a waiting period will be scheduled ahead of the reported lower priority

traffic. Therefore, employing fixed bandwidth allocation increases frame delay for AF and BE traffic since the allocated bandwidth is mostly used for EF traffic. The aforementioned problem is called the light load penalty which can be solved by two strategies proposed in [8]. The first tactic uses two-stage buffers. A priority queue and a first in first out (FIFO) queue inform the first and second stage, respectively. Transmitting traffic from the ONU side at the allocated transmission window starts from the second stage while the first stage forwards traffic to the second one in a priority order. At the end of the time slot, ONU sends a REPORT message to the OLT based on the current occupancy of its second stage buffer. This approach mitigates the light load penalty problem at the sacrifice of the increase in delay for higher priority traffic (i.e., EF traffic). The second tactic is called the credit-based slot sizing that requires some prediction methods [14]. Each ONU knows how much data will arrive in the next specific interval, and the size of the granted slot will be increased by the amount of anticipated additional data. It should be noted that the anticipation is done for constant bit rate (CBR) flows (e.g., EF traffic). Research by Zhang and Ansari [55] supports the fairness in bandwidth allocation among applications with different QoS requirements in EPON. The aforementioned differentiated service provisions some queues with higher QoS over others. However, Diffserv can hardly meet any specific QoS requirements imposed by diversified applications in EPON. Brooks and Hestnes [13] defined application utilities to quantify users quality of experience (QoE) as a function of network layer QoS metrics. The fair resource allocation issue is formulated as a utility max-min optimization problem and the optimal value can be achieved by proper bandwidth allocation and queue management.

1.4 Energy-efficient Access Networks

A variety of bandwidth-hungry applications and services such as high-definition television, video streaming, and social networking [52, 47, 30] are rapidly being deployed, thus leading to a continuous surge in bandwidth demand across networking infrastructure, notably the access portion. Thus, both wireline and wireless telecommunications operators are driven to upgrade their access networks to provide broader bandwidth for their subscribers [46, 18]. To provision a higher data rate, more power will be consumed in network devices to facilitate faster data processing. Besides, high-speed data processing incurs fast heat buildup and

high heat dissipation, which further incur high energy consumption for cooling. Baliga *et al.* [9] estimated that the access network energy consumption increases linearly with the provisioned data rate.

In order to mitigate global warming and to control the operational expenses, energy efficient solutions become essential. Using energy in an efficient manner for all networks is challenging and is considered as an important and vital concern. The ever increase of broadband users has drawn global attention to reduce energy consumption in data communication networks [16, 20, 7]. Optical access networks consume a significant amount of energy of communications infrastructure due to the large number of access nodes. However, owing to the proximity of optical fibers to end users and the passive nature of remote nodes, passive optical networks (PONs) consume the smallest energy per transmission bit among various access technologies including WiMAX, FTTN, and point to point optical access networks [31, 55, 61, 60]. Nevertheless, it is still desirable to further reduce energy consumption of PONs since every single watt saving will end up with overall terawatt and even larger power saving as PON is deployed worldwide.

To provide higher data rates to meet end users increasing bandwidth demands in the future, access networks will upgrade their provisioning capacity and correspondingly experience further increase of energy consumption. Therefore, reducing energy consumption of PONs becomes even more imperative for the 10G EPON system which provides ten times of the data rate of the 1G EPON system because large data rate provisioning requires high power consumption of both the optical and electrical components of various devices.

1.4.1 Energy-efficient Strategies in PONs

The process of designing and controlling capacity adaptive access networks is challenging. Optical access networks need to be equipped with rate-variable transmitters and receivers. Since optical transceivers are usually operated at a single data rate, rate-variable transceivers are not readily available. Essentially, multiple transceivers with the same functionality but operating at different rates need to be equipped, and this incurs high capital expenditure (CAPEX). The other challenging issue is that a high-capacity network provides better network performances such as low delay and small packet loss, and accordingly achieves high

user quality of service/experience. In other words, a low-capacity network may incur large delay and high packet loss ratio, and therefore degraded network services. From the network performances point of view, it is desired to minimize the network energy consumption without degrading user services.

There are two strategies to reduce power consumption of network devices. First is to adapt transmitting/receiving data rates of devices to the real-time incoming traffic rate, and second is to minimize the power consumption for any given transmitting or receiving data rate [22]. Reducing the overall power consumption can be done by putting devices in the sleep mode whenever they are idle, controlling output signal power properly, and equipping the network with a set of devices with the same functionality, but operating at different data rates.

In the optical network, it is feasible to equip OLT and ONUs with both low-rate and high-rate devices. When the network is lightly loaded the devices operate in low rates; otherwise, the devices operate at high rates. Hence, rate-variable network nodes provision different data rates with different power consumptions. However, owing to the shared-media nature, changing the rate of one network node will affect the bandwidth received by other network nodes which share the same media [56].

Employing the sleep and/or doze mode is also considered as an effective approach to reduce the EPON power consumption. Since the ONUs do not send and receive traffic 24 hours a day, putting the optical devices in the sleep mode whenever the network is lightly loaded is a practical and simple method to save as much as 93.75% or 96.875% of the energy [41, 22]. However, a proper sleep mode control protocol is needed to make OLT aware of sleep status of the ONUs to avoid missing the downstream traffic.

CHAPTER 2

STANDARDS-COMPLIANT EPON SLEEP CONTROL

Previously, in order to decrease the energy consumption, defining the sleep mode was proposed for idle ONUs [51]. Since traffic of ONUs is rather bursty and changes dynamically [34], putting ONUs into the sleep mode when the ONU does not have downstream or upstream traffic can save a significant amount of ONU energy [29, 51]. According to [57], a multi power level ONU is defined based on the energy consumption of the working part. In the mentioned scheme, the transmitter and receiver can go to the sleep mode separately. However, the transition between the states with all active/awake parts and the receiver being totally asleep actually do not exist since an ONU needs to receive some downstream control packets to perform upstream transitions. Regarding EPON ONUs, the sleep control of transmitters inside ONUs is relatively easier than that of receivers since the arrival of the upstream traffic can trigger the wakeup of asleep transmitters. Ideally, an ONU is desired to stay in the sleep mode with low power consumption when the ONU does not have traffic, and switch back into the active mode when traffic of an ONU arrives. However, the broadcast nature of the EPON downstream transmission disallows an ONU entering the sleep mode. As shown in Figure 2.1, the downstream data traffic of EPON ONUs are TDM multiplexed onto a single wavelength, and broadcasted to all ONUs [37]. An ONU has to receive and check all downstream packets, and then decides whether the packets are destined to itself. Since all incoming downstream packets have to be checked, an ONU needs to stay awake all the time to avoid missing its downstream traffic. Formerly, the sleep mode was proposed to be enabled in optical network units (ONUs) to reduce their power consumption. To avoid service disruption, asleep ONUs should wake up upon the arrival of downstream or upstream traffic. However, it is challenging to wake up asleep ONUs when downstream ONU traffic arrives in Ethernet PON. Without proper sleep-aware MAC control, receivers at ONUs need to be awake all the time to avoid missing their downstream packets. A number of schemes have been proposed to address the downstream challenge so as to reduce the energy consumption of ONUs. These proposed energy saving schemes can be

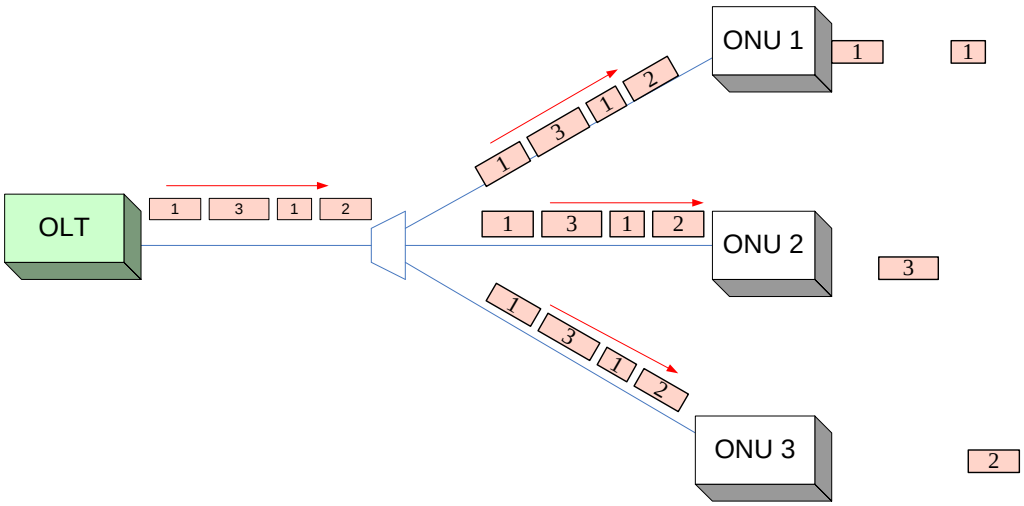

Figure 2.1 Downstream transmission in EPON.

divided into two major classes. The first class tries to design a proper MAC control scheme to convey the downstream queue status to ONUs, while the second class focuses on investigating energy-efficient traffic scheduling schemes. The two-way or three-way handshake processes performed between the OLT and ONUs are examples of schemes of the first class [41]. Yan *et al.* [54] proposed two downstream scheduling algorithms in order to save the energy in EPON. In the first algorithm, downstream centric scheme (DCS), the OLT buffers the downstream traffic for a specific ONU and will send to it during the prescheduled time slot for upstream traffic. In the second algorithm, upstream centric scheme (UCS), the proper time slot is not only scheduled for upstream traffic but also determined for downstream traffic. More specifically, both upstream and downstream traffic in UCS could trigger the ONU to switch the status from sleep to active, and hence higher delay would be imposed to the system. Typically, in the first class schemes, the OLT sends a control message notifying an ONU that its downstream queue is empty; the ONU optionally enters the sleep mode and then sends a sleep acknowledgement or negative acknowledgement message back to the OLT. While the OLT is aware of the sleep status of ONUs, it can buffer the downstream arrival traffic until the sleeping ONU wakes up. However, to implement the handshake process, the EPON MAC protocol, multipoint control protocol (MPCP) defined in IEEE 802.3ah or IEEE 802.3av, has to be modified to include new MPCP protocol data units (PDUs). In addition, the negotiation process takes at least several round trip times, implying that an ONU has to wait for several round trip times before entering the sleep status after it

infers that its downstream queue is empty. This may significantly impair the energy saving efficiency.

Energy saving schemes of the second class tackle the downstream challenge by designing suitable downstream bandwidth allocation schemes. Formerly, Lee *et al.* [33] proposed to implement fixed bandwidth allocation (FBA) in the downstream when the network is lightly loaded. By using FBA, the time slots allocated to each ONU in each cycle are fixed and known to the ONU. Thus, ONUs can go to sleep during the time slots allocated to other ONUs. However, since traffic of an ONU dynamically changes from cycle to cycle, FBA may result in bandwidth under- or over-allocation, and consequently degrade services of ONUs in some degree. Yan *et al.* [53] proposed to schedule the downstream traffic and the upstream traffic simultaneously. Since the downstream traffic of an ONU is sent over the time slots that its upstream traffic is sent, the ONU stays in the awake status during that time period and will not miss its downstream packets. This scheme works well when traffic in the upstream and downstream are symmetric, but it may cause inefficient bandwidth utilization when the downstream traffic outweighs upstream traffic.

2.1 Main Contributions

In this Chapter, the problem of reducing energy consumption of optical access networks are studied. An efficient sleep control scheme, which possesses two main advantages, is presented. First, it belongs to the second class, and hence can efficiently put ONUs into sleep without modifying the EPON MAC protocol. Also, since it does not require handshaking between OLT and ONUs, the proposed scheme can achieve high energy saving efficiency. Second, the proposed scheme allows dynamic bandwidth allocation among ONUs. Consequently, it achieves high bandwidth utilization. Specifically, our main contributions are:

- A simple and efficient sleep control scheme to tackle the downstream challenge is proposed, and it can efficiently put ONU receivers into sleep without modifying the standardized EPON MAC protocol. The proposed scheme contains two main parts: downstream traffic scheduling rules at the OLT and sleep control schemes at ONUs. By letting ONUs be aware of the downstream traffic scheduling rules, ONUs can infer their own downstream queue status and switch into the sleep status properly; by letting OLT know the sleep control scheme implemented at ONUs, the OLT can accurately infer the sleep status of ONUs and buffer traffic of asleep ONUs accordingly (Section 2.2).

- A semi-Markov chain model is described to theoretically analyze delay and energy saving performances of the proposed sleep control scheme (Section 2.3).
- Numerical results and simulation results show that with proper settings of sleep control parameters, the proposed scheme can save as high as 50% of the ONU receiver energy (Section 2.4).

2.2 Design of a Sleep Control Scheme

Rather than focusing on enabling the sleep mode of transmitters and receivers at the same time [54], this chapter targets at addressing the downstream challenge only. The proposed scheme can be applied when transmitters and receivers can be independently put into sleep [57]. Another application scenario is when the ONU has downstream traffic only, e.g., file downloading and broadcast TV applications. In Chapter 3, the proposed scheme will be combined with the upstream traffic scheduling scheme such that both receivers and transmitters can be put into the sleep mode simultaneously.

The main idea can be generalized as follows. First, we set certain downstream traffic scheduling rules at OLT and let the rules be known to ONUs. Since an ONU owns the information of the downstream traffic scheduling rules, it can infer its current downstream queue status based on historical arrival downstream traffic. Second, according to the inferred queue status, ONUs make their own sleep decisions based on some sleep control rules. These sleep control rules implemented at the ONU side is also known to the OLT. Third, based on the sleep control rules, the OLT infers the status of ONUs, and buffers the incoming downstream traffic of asleep ONUs accordingly. Essentially, the *downstream traffic scheduling rules*, the *downstream queue inference at ONUs*, the *sleep control rules*, and the *ONU sleep status inference at the OLT* constitute four key components of the proposed sleep control scheme.

2.2.1 Downstream Traffic Schedule Rule

Traffic scheduling in both downstream and upstream are not specified in the EPON standards IEEE 802.3ah and IEEE 802.3av. Upstream bandwidth allocation has received extensive research attention in the past years. For upstream scheduling, efficient upstream bandwidth utilization requires the OLT to allocate the bandwidth based on queue reports from ONUs.

The time gap between the traffic report and the bandwidth grant process may incur inefficient utilization of upstream bandwidth.

Utilizing the time gap for high network resource utilization has been a key objective in designing bandwidth allocation algorithms for the upstream. Different from the upstream transmission, the downstream transmission does not have the queue report and bandwidth grant process since downstream traffic is queued at the OLT, which also makes the downstream traffic scheduling decisions. As IEEE 802.3ah and IEEE 802.3av standards do not specify a dynamic bandwidth allocation scheme for downstream scheduling or upstream scheduling, having a fixed downstream traffic scheduling cycle does not violate the EPON standard. Thus, in designing the downstream traffic scheduling rules, our main objective is to facilitate ONUs infer their own downstream traffic status, rather than maximizing the bandwidth utilization. Below are the designed downstream traffic scheduling rules.

- *Rule 1*: Define the time duration of 2 ms as the downstream traffic scheduling cycle.
- *Rule 2*: In a scheduling cycle, each ONU is allocated with some time durations if it has downstream traffic. Note that ONUs do not have to be allocated with continuous time durations within a scheduling cycle.
- *Rule 3*: If the OLT infers that an ONU is sleeping, it queues the arrival downstream traffic of the ONU until the ONU wakes up.

The reason for setting the scheduling cycle as 2 ms is to guarantee delay and jitter performances of delay-sensitive applications such as voice and video. The purpose of Rule 2 is to help an ONU infer its downstream queue status. Besides, this rule also helps prevent ONUs from being starved. Rule 3 is to avoid asleep ONUs from missing their downstream packets.

2.2.2 Downstream Traffic Inference at ONU

According to the downstream traffic scheduling rules, if an ONU fails to receive any downstream data traffic within an EPON traffic scheduling cycle, the ONU can infer that its downstream queue is empty. Thus, rather than being explicitly notified by the OLT about its downstream queue status, an ONU can infer its downstream queue status simply by monitoring the downstream bandwidth allocated among ONUs.

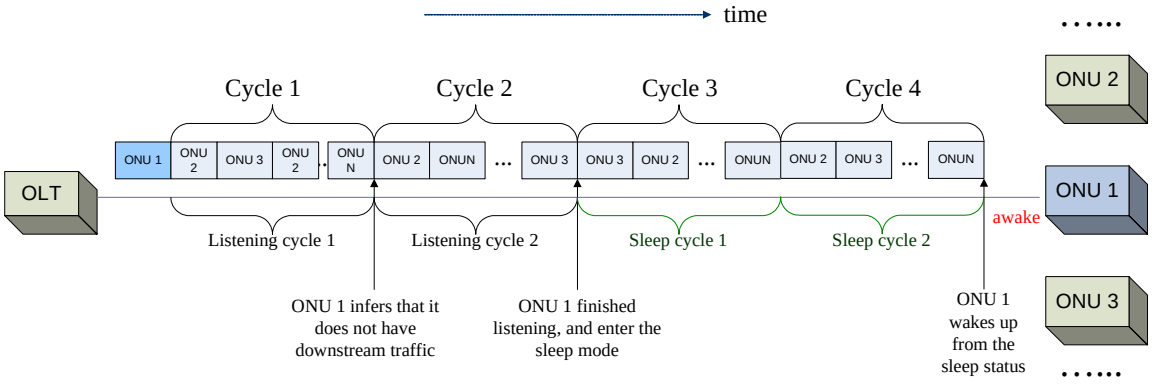

Figure 2.2 The sleep control at ONU.

2.2.3 Sleep Control Rules

After being aware that its downstream queue is empty, an ONU can choose to enter the sleep mode. The following sleep control rules are designed.

"*If an ONU does not receive downstream data traffic for x traffic scheduling cycles, it switches into the sleep state, and sleeps for y traffic scheduling cycles.*"

x traffic scheduling cycles are referred to as listening cycles, and y traffic scheduling cycles are referred to as sleeping cycles. Both x and y are known to the OLT such that the OLT can infer the sleep status of ONUs.

Figure 2.2 shows an example of the sleep control rules with $x = 2$ and $y = 2$. At the end of cycle 1, ONU 1 observes that it is not allocated with any time slots during the entire cycle of cycle 1. At that moment, ONU 1 infers that its downstream queue is empty. Since the number of listening cycles equals to 2, ONU 1 continues listening to the channel for one more cycle. At the end of cycle 2, ONU 1 still does not receive any downstream traffic. Then, it switches into the sleep status and sleeps for two cycles since the number of sleeping cycles equals to 2. After cycle 4, ONU 1 wakes up from the sleep status.

2.2.4 ONU Status Inference and Traffic Scheduling at OLT

To avoid missing the downstream traffic when an ONU is sleeping, the OLT should be aware of the sleep status of the ONU, and then buffer its incoming downstream traffic until the ONU wakes up. To enable the ONU status be accurately inferred by the OLT, we let the OLT own the information of the sleep control algorithm implemented at each ONU. Owing to the fact that an ONU makes its sleep decision based on the downstream bandwidth allocation

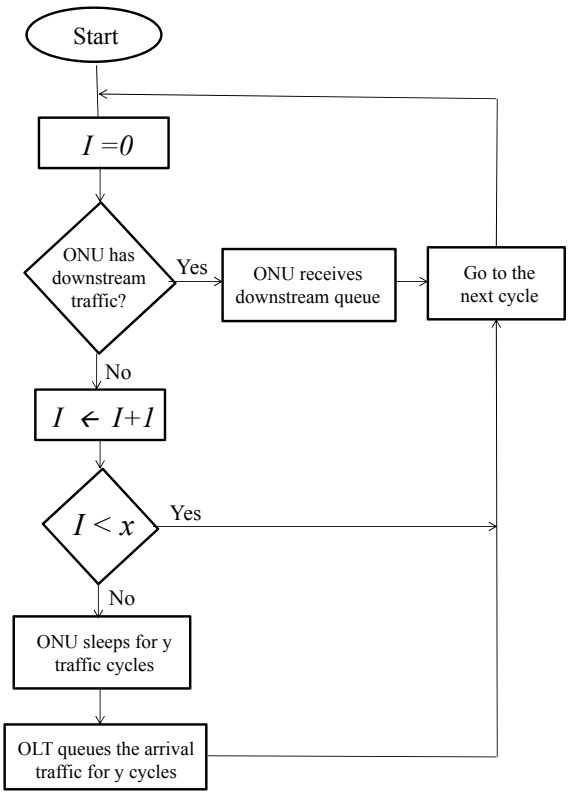

Figure 2.3 Flow chart of the sleep control scheme implemented at both OLT and ONUs.

profile which is also known to the OLT, the OLT can accurately infer the status of each ONU at any time. The ONU status inference can be described as follows.

"*If the OLT does not allocate any time slots to an ONU for x traffic scheduling cycles, the ONU will enter the sleep status in the next y traffic scheduling cycles.*"

After the OLT infers that an ONU is sleeping, the OLT buffers the arrival downstream traffic of this ONU until the ONU wakes up from sleep.

Figure 2.3 illustrates a flow chart of the proposed sleep control scheme. Indicator $"I"$ counts the number of cycles in which no downstream packets are scheduled for the specific ONU. By the time I reaches x, the ONU makes the sleep decision. The OLT is aware of the sleep control algorithm implemented at each ONU. Therefore, the OLT infers the sleep status of each ONU based on the traffic scheduled to each ONU. The OLT buffers the arrival downstream traffic of the ONU during the sleep cycles. Once the OLT finds that an ONU changes its status, the OLT adjusts its traffic scheduling scheme accordingly.

According to the proposed scheme, it is not necessary for the OLT and ONUs to have identical view of the scheduling cycles. Each of them can view the timestamp of the first bit of its received traffic as the beginning of its cycle. Based on the above described schemes,

ONUs can switch into the sleep mode without modifying the EPON control protocol. The listening time duration of x cycles and the sleep time duration of y cycles determine the energy saving efficiency and quality of service (QoS) performances. Proper setting of x and y needs to consider energy efficiency and QoS of user sessions. In our previous work [57], we described an example in which $x = 1$ and y exponentially increases with the time duration that an ONU's downstream queue remains empty. In this Chapter, the focus is on investigating the impact of x and y on network performances and energy efficiency under different traffic loads. Analytical results below will provide insights on proper settings of x and y for different traffic loads.

2.3 System Model and Performance Analysis

In this section, semi-Markov chains to theoretically analyze the delay and energy saving performances of the sleep control scheme are employed. For ease of analysis, Poisson traffic arrival is considered. We assume the downlink packet arrival is a Poisson process with the average rate λ packets/s, and the packet arrival process is independent from the distribution of the packet size. Let N be the number of ONUs and R bits/s be the rate of the downlink channel. Then, each ONU is serviced with the rate of R/N bits/s. The service time of each packet, i.e., packet size/(R/N), is assumed to be exponentially distributed with average value of $1/\mu$. Regarding the transit time between the sleep status and awake status, Wong *et al.* [50] proposed two ONU architectures to reduce the recovery overhead into tens of nanoseconds, which are negligible as compared to the duration of a traffic scheduling cycle. In this work, the transit time is not considered.

2.3.1 ONU State and State Transitions

In the Markov chain model, each ONU has three possible sets of states: active states $\{\mathbb{A}(i)\}_{i=0}^{+\infty}$, listening states $\{\mathbb{L}(j)\}_{j=1}^{x}$, and sleeping state $\mathbb{S}$.

- $\mathbb{A}(i)$ refers to the state that an ONU has i queued downstream packets by the end of a traffic scheduling cycle. There is no upper bound of i as the buffer size is assumed to be infinite.
- $\mathbb{L}(j)$ refers to the state that an ONU does not have any downstream packets, and has not received any downstream data traffic for j traffic scheduling cycles. The listening time duration can be as large as x traffic scheduling cycles, where x is the number of listening cycles.

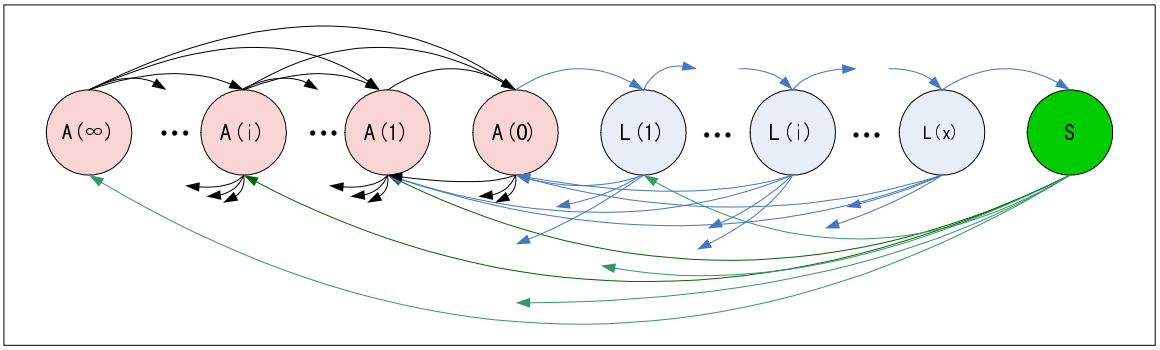

Figure 2.4 State transitions in the Markov Chain.

- $\mathbb{S}$ refers to the status that the ONU stays asleep. The sleep time duration equals to y traffic scheduling cycles, where y is the number of sleeping cycles.

Figure 2.4 illustrates the state transitions. For a given ONU, assume the number of queued packets equals to α. If $\alpha > 0$, the ONU stays in state $\mathbb{A}(\alpha)$. If $\alpha = 0$, the ONU could possibly stay in the active state $\mathbb{A}(0)$, listening states $\{\mathbb{L}(j)\}_{j=1}^{x}$, or the sleeping state $\mathbb{S}$. During any traffic scheduling cycle, i packets may arrive and j packets may depart for any ONU. There are three main cases of i and j.

- If j is smaller than i, the number of queued packets is increased by $j - i$ at the end of the cycle.
- If j is greater than i, the number of queued packets is decreased to either $\alpha - (j - i)$ if $\alpha > j - i$, or 0 otherwise.
- If no packet arrives during a traffic scheduling cycle, i.e., $i = 0$, the ONU state transits from $\mathbb{A}(0)$ to $\mathbb{L}(0)$ if the ONU stayed in state $\mathbb{A}(0)$ in the former cycle, from $\mathbb{L}(k)$ to $\mathbb{L}(k+1)$ if the ONU stayed in state $\mathbb{L}(k)$ in the former cycle, and from $\mathbb{L}(x)$ to $\mathbb{S}$ if the ONU stayed in state $\mathbb{L}(x)$ in the former cycle.

Denote $p^a(\beta, \gamma)$ and $p^d(\beta, \gamma)$ as the probability that β downstream packets arrive at the OLT and depart from the OLT during γ traffic scheduling cycles, respectively. The probability that i packets arrive and j packets depart from the downstream queue equals to $p^a(i, \gamma) \cdot p^b(j, \gamma)$. Then,

- State transitions from $\mathbb{A}(0)$ to $\mathbb{L}(1)$, from $\mathbb{L}(k)$ to $\mathbb{L}(k+1)$, or from $\mathbb{L}(x)$ to $\mathbb{S}$ happen when no packets arrive during the traffic scheduling cycle. The probability of each case equals to $p^a(0, 1)$.
- State transition from $\mathbb{L}(j)$ to $\mathbb{A}(k)$ occurs when the number of arrival packets is greater than the number of departure packets by k during the traffic scheduling cycle. The probability equals to $\sum_{i=0}^{+\infty} p^a(k+i, 1) \cdot p^d(i, 1)$.

- State transition from $\mathbb{A}(i)$ to $\mathbb{A}(i-k)$ happens when the number of arrival packets is smaller than the number of departure packets by k. The probability equals to $\sum_{j=0}^{+\infty} p^d(k+j,1) \cdot p^a(j,1)$.
- State transition from $\mathbb{S}$ to $\mathbb{A}(i)$ happens when i packets arrive during y sleeping cycles. The probability equals to $p^a(i,y)$.
- State transition from $\mathbb{S}$ to $\mathbb{L}(1)$ occurs when no packets arrive during y sleeping cycles. The probability equals to $p^a(0,y)$.

Based on the assumptions of Poisson arrival traffic, $p^a(\beta,\gamma)$ and $p^d(\beta,\gamma)$ can be obtained as follows.

$$p^a(\beta,\gamma) = e^{-\lambda\gamma T} \cdot (\lambda \cdot \gamma T)^\beta / \beta! \tag{2.1}$$

$$p^d(\beta,\gamma) = e^{-\mu\gamma T} \cdot (\mu \cdot \gamma T)^\beta / \beta! \tag{2.2}$$

where T is the duration of a traffic scheduling cycle. After having derived the state transition probabilities, we can obtain the steady state probability of each state, and thus analyze the energy saving and delay performances of our proposed sleep control scheme.

2.3.2 Steady State Probability

Consider $P(\mathbb{S})$, $\{P(\mathbb{A}(i))\}_{i=0}^{\infty}$, $P(\mathbb{L}(j))\}_{j=1}^{x}$ as the probability of each ONU state when the network is at its steady state. Then, these steady state probabilities satisfy the following constraints.

$$\begin{aligned} P(\mathbb{S})[\sum_{i=1}^{\infty} pr\{\mathbb{S} \to \mathbb{A}(i)\} + pr\{\mathbb{S} \to \mathbb{L}(1)\}] \\ = P(\mathbb{L}(x)) pr\{\mathbb{L}(x) \to \mathbb{S}\} \end{aligned} \tag{2.3}$$

Equation 3 shows the steady state probability of the sleep state. State $\mathbb{S}$ can be reached only via state $\mathbb{L}(x)$. State transition from $\mathbb{S}$ to the other states depends on the number of arrival packets during the traffic scheduling cycle. No arrival packet causes a transition to the state $\mathbb{L}(1)$.

$$\begin{aligned} P(\mathbb{L}(x))[\sum_{i=0}^{\infty} pr\{\mathbb{L}(x) \to \mathbb{A}(i)\} + pr\{\mathbb{L}(x) \to \mathbb{S}\}] \\ = P(\mathbb{L}(x-1)) pr\{\mathbb{L}(x-1) \to \mathbb{L}(x)\} \end{aligned} \tag{2.4}$$

Steady state probability for all the listening states except $\mathbb{L}(1)$ and $\mathbb{L}(x)$ are the same as follows:

$$P(\mathbb{L}(j))[\sum_{i=0}^{\infty} pr\{\mathbb{L}(j)\rightarrow\mathbb{A}(i)\} + pr\{\mathbb{L}(j)\rightarrow\mathbb{L}(j+1)\}]$$
$$= P(\mathbb{L}(j-1))pr\{\mathbb{L}(j-1) \rightarrow \mathbb{L}(j)\}(1 < j < x) \tag{2.5}$$

$$P(\mathbb{L}(1))[\sum_{i=0}^{\infty} pr\{\mathbb{L}(1) \rightarrow \mathbb{A}(i)\} + pr\{\mathbb{L}(1) \rightarrow \mathbb{L}(2)\}]$$
$$= P(\mathbb{A}(0))pr\{\mathbb{A}(0) \rightarrow \mathbb{L}(1)\} + P(\mathbb{S})pr\{\mathbb{S} \rightarrow \mathbb{L}(1)\} \tag{2.6}$$

$$P(\mathbb{A}(i))\sum_{j\neq i} pr\{\mathbb{A}(i)\rightarrow\mathbb{A}(j)\}=\sum_{j\neq i} P(\mathbb{A}(j))pr\{\mathbb{A}(j)\rightarrow\mathbb{A}(i)\}$$
$$+\sum_{j\neq i} P(\mathbb{L}(j))pr\{\mathbb{L}(j)\rightarrow\mathbb{A}(i)\}+ P(\mathbb{S})pr\{\mathbb{S}\rightarrow\mathbb{A}(i)\} \tag{2.7}$$

$$P(\mathbb{A}(0))[\sum_{i\neq 0} pr\{\mathbb{A}(0) \rightarrow\mathbb{A}(i)\} + pr\{\mathbb{A}(0) \rightarrow \mathbb{L}(1)\}] =$$
$$\sum_{i\neq 0} P(\mathbb{A}(i))pr\{\mathbb{A}(i)\rightarrow\mathbb{A}(0)\}+\sum_{j\neq i} P(\mathbb{L}(j))pr\{\mathbb{L}(j)\rightarrow\mathbb{A}(0)\} \tag{2.8}$$

Additionally, the sum of the probabilities of all states should equal to 1, i.e.,

$$P(\mathbb{S}) + \sum_{i=0}^{+\infty} P(\mathbb{A}(i)) + \sum_{j=1}^{x} P(\mathbb{L}(j)) = 1 \tag{2.9}$$

The steady state probabilities can thus be obtained by solving the above Equations (2.3)-(2.9).

2.3.3 Performance Analysis

Power Saving Denote $P(\mathbb{S})$, $\{P(\mathbb{A}(i))\}_{i=0}^{\infty}$,and $P(\mathbb{L}(j))\}_{j=1}^{x}$ as the probability of each ONU state when the network reaches its steady state. Denote $W(\mathbb{A})$, $W(\mathbb{L})$, and $W(\mathbb{S})$ as the power consumption when an ONU is in the active, listening, and sleep state, respectively. Then, since the time duration of these states are 1 cycle, 1 cycle, and y cycles, respectively, the energy consumption in these three states are $W(\mathbb{A})$, $W(\mathbb{L})$, and $y \cdot W(\mathbb{S})$, respectively.

The average energy consumption equals to

$$W(\mathbb{A})\cdot\sum_{i=0}^{\infty}P(\mathbb{A}(i))+W(\mathbb{L})\cdot\sum_{j=1}^{x}P(\mathbb{L}(j))+y\cdot W(\mathbb{S})\cdot P(\mathbb{S}) \tag{2.10}$$

Extra Delay Denote $E[\delta|\mathbb{S}]$, $E[\delta|\mathbb{L}]$, and $E[\delta|\mathbb{A}]$ as the conditional expectation of the delay for the packets which arrive when an ONU is sleeping, listening, and active, respectively. Then, the average delay equals to

$$E[\delta|\mathbb{S}]\cdot P(\mathbb{S})+E[\delta|\mathbb{L}]\cdot\sum_{j=1}^{\infty}P(\mathbb{L}(j))+E[\delta|\mathbb{A}]\cdot\sum_{i=0}^{\infty}P(\mathbb{A}(i)) \tag{2.11}$$

For packets which arrive when an ONU is sleeping, they have to wait until an ONU wakes up from the sleep status before being transmitted. The average waiting time equals to $y/2$ cycles since the sleep time duration equals to y cycles. We refer to this delay as "wait-to-wakeup" delay. In addition, a packet has to wait until the completion of the transmission of all other packets arrived prior to its arrival. For the jth packet arrival when an ONU is sleeping, it has to wait for the transmission of all the first $j-1$ packets. Since on average each packet takes $1/\mu$ time to be transmitted, the average waiting time for the jth packet equals to $(j-1)\cdot 1/\mu + y/2\cdot T$. For the case that there are k arrival packets when an ONU is asleep, the average delay of these k packets equals to $\frac{\sum_{j=1}^{k}(j-1)\cdot 1/\mu+y/2\cdot T}{k} = \frac{(k-1)}{2}\cdot 1/\mu + \frac{y}{2}\cdot T$. We refer to this delay as "queuing delay". We can further derive the conditional expectation of the delay for packets which arrive when an ONU is sleeping.

$$E[\delta|\mathbb{S}] = y/2\cdot T + \sum_{i=1}^{\infty}[p^a(i,y)(i-1)\cdot 1/\mu] \tag{2.12}$$

For packets which arrive when an ONU is in the active status or listening status, they do not need to wait until an ONU wakes up, and thus do not experience "wait-to-wakeup" delay. Considering the queuing delay, the average waiting time for these packets is

$$E[\delta|\mathbb{L}] = \sum_{i=1}^{\infty}[p^a(i,x)(i-1)\cdot 1/\mu] \tag{2.13}$$

$$E[\delta|\mathbb{A}] = \sum_{i=1}^{\infty}[p^a(i,z)(i-1)\cdot 1/\mu] \tag{2.14}$$

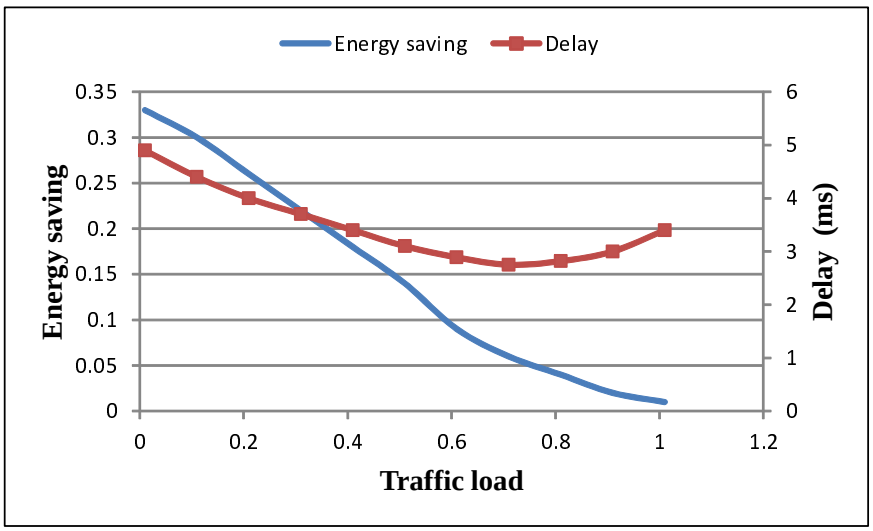

Figure 2.5 Energy saving and delay vs. traffic load for Poisson traffic.

x in Equation (2.13) and z in Equation (2.14) represent a traffic scheduling cycle in the listening and active state, respectively.

2.4 Numerical Results for the Markov Model

To obtain the numerical results, it is assumed that a 1G EPON supports 32 ONUs. Traffic scheduling cycle is considered as $2ms$, and each ONU is serviced with the rate of $\frac{1}{32}Gb/s$. Since ONUs do not share resources among each other in the model, we analyze a single ONU behavior. As the recovery time is neglected in comparison to the duration of the traffic scheduling cycle, the proposed ONU architecture in [51] can be exploited. Thus, the power consumption of the ONU receiver in the active and sleep status are selected as 3.85 W and 1.28 W, respectively. As for the listening status, clearly the power consumption has to be within the range of $[1.28, 3.85]$. Since the exact number from publicly available literature cannot be retrieved, simulations are conducted using different values for the power consumption of the ONU receiver in the listening status. The results are shown using 2.5, but the observations and conclusions can be similarly drawn for other values.

Figure 2.5 illustrates the energy saving performances under different traffic arrival rates. The results are obtained by considering 1 cycle duration for listening and 2 cycles for sleep periods. The traffic load $(\frac{\lambda}{\mu})$ increases from 0.01 to 1. As the arrival traffic rate

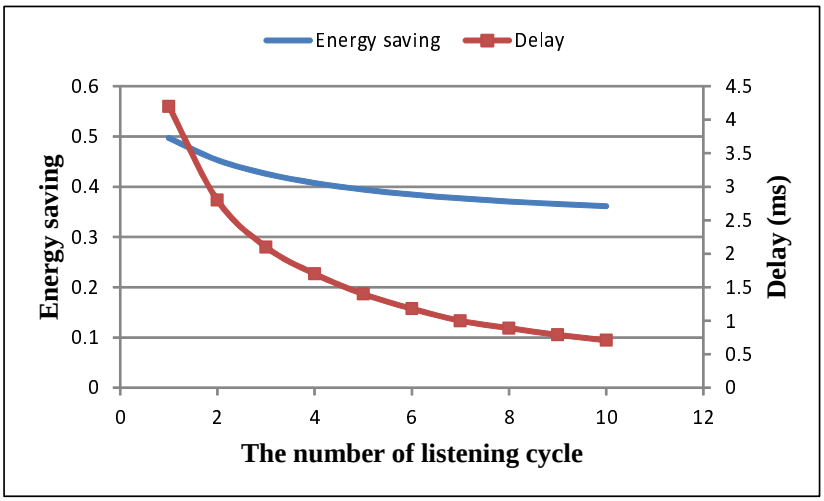

Figure 2.6 Energy saving and delay vs. the number of listening cycles for Poisson traffic.

increases, both the sleep state probability and listening state probability decrease, and thus the energy saving decreases.

The definition of the "wait-to-wakeup" delay is introduced to facilitate the analysis of delay performance. For packets which arrive when an ONU is sleeping, they have to wait until an ONU wakes up from the sleep status before being transmitted. The average waiting time equals to $y/2$ cycles since the sleep time duration equals to y cycles. We refer to this delay as the "wait-to-wakeup" delay.

Regarding delay performances, when the traffic rate is small, the queuing delay is small, and the average delay is dominated by the "wait-to-wakeup" time. When the traffic rate increases beyond some certain value, the probability that an ONU stays in the sleep status is small, and the "wait-to-wakeup" time takes a small portion of the overall average delay. Thus, the average delay is dominated by the queuing delay when the traffic rate is large enough. Figure 2.5 shows that the delay first decreases with the increase of the traffic rate. This is because the overall average delay is dominated by the "wait-to-wakeup" time in this case. With the increase of the traffic rate, the sleep state probability decreases, and the "wait-to-wakeup" time decreases, therefore resulting in the decrease of the average delay. Figure 2.5 also shows that delay increases when the traffic rate increases beyond some point. In this case, delay is dominated by the queuing delay. With the increase of the traffic rate, the queuing delay increases, and thus the average delay increases.

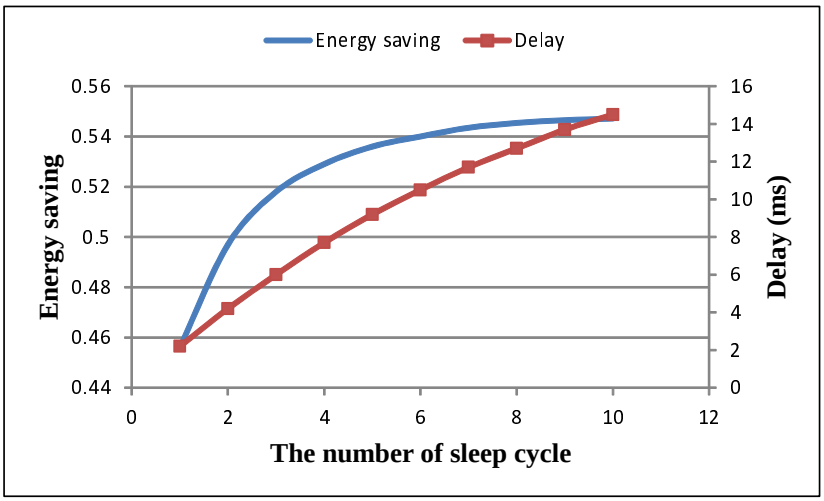

Figure 2.7 Energy saving and delay vs. the number of sleep cycles for Poisson traffic.

Figure 2.6 illustrates the impact of the listening time duration x on the energy saving and delay by fixing traffic load as 0.147 while the number of sleep cycles y equals to 2 cycle. With the increase of the listening cycles x, the probability that an ONU stays in the listening state increases, and the probability that an ONU stays in the sleep state decreases. Thus, the ONU stays awake for a longer time and the energy saving decreases.

For delay performances, delay decreases with the increase of the listening time owing to the decrease of the sleep state probability. As stated before, because of the "wait-to-wakeup" time, packets experience longer delay if they arrive when an ONU stays in the sleep status as compared to those arrive when an ONU stays in the active and listening status. Thus, the decrease of the sleep state probability results in the decrease of the average packet delay.

Figure 2.7 shows the impact of the number of sleeping cycles y on the performances while the number of listening cycles x equals to 2 and the traffic load is set to 0.147. With the increase of the number of sleeping cycles y, the energy saving increases since the energy consumption in the sleep status is the smallest among all three sets of states. As it can be seen, when the number of sleep cycles equals to 10, the energy saving is as large as 55%. On the other hand, with the increase of y, the probability that an ONU stays in the sleep status decreases. Thus, the rate of the energy saving is slower than that of the sleep time duration.

Regarding delay performances, delay increases with the increase of the sleep time since longer "wait-to-wakeup" time will be incurred with larger sleeping time. The delay almost

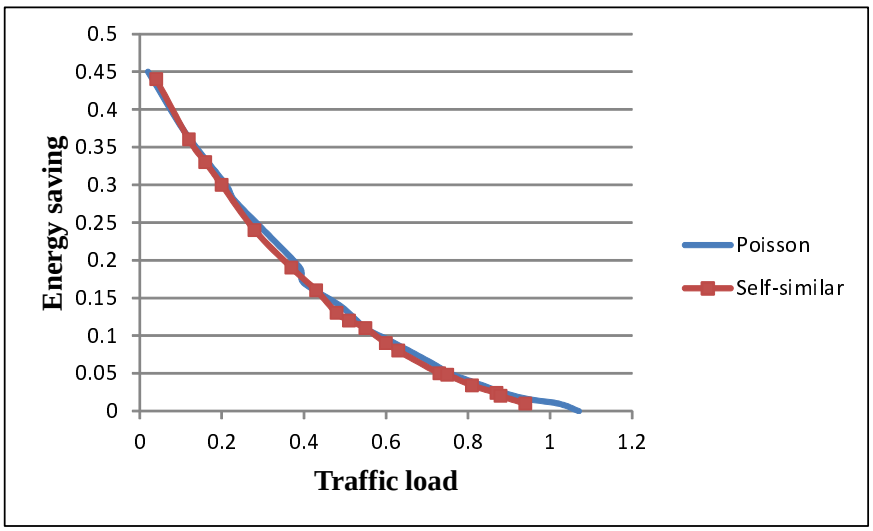

Figure 2.8 Energy saving vs. traffic load for Poisson and self-similar traffic.

increases linearly with the increase of the sleep time because the "wait-to-wakeup" time dominates the overall delay and increases linearly with the number of sleeping cycles y.

2.5 Simulation Model and Results

In this section, the performances of the sleep control scheme for Poisson and non-Poisson traffic is studied using simulations. Consider a 1G EPON system supporting 32 ONUs. The downstream traffic scheduling cycle duration equals to $2ms$. Since self-similarity is exhibited in many applications, in this dissertation, the results of Poisson traffic is compared with self-similar traffic. In the self-similar traffic, each ONU receives self-similar traffic [24] with the Hurst parameter of 0.8. The packet length is uniformly distributed between 64 bytes to 1518 bytes. The downstream traffic scheduling is as follows. If the total queued traffic in a cycle is less than the maximum value which can be accommodated by the cycle, all the packets being queued are scheduled; otherwise, the bandwidth allocated to each ONU is proportional to its requested bandwidth.

Figures 2.8 and 2.9 show the system performances under different traffic load. Here, "load" is defined as the ratio between the total arrival traffic and the network capacity. To compare the results with the numerical analysis, we follow the same setting for the parameters, $x = 1$ and $y = 2$. It can be seen that the trend of energy saving and delay

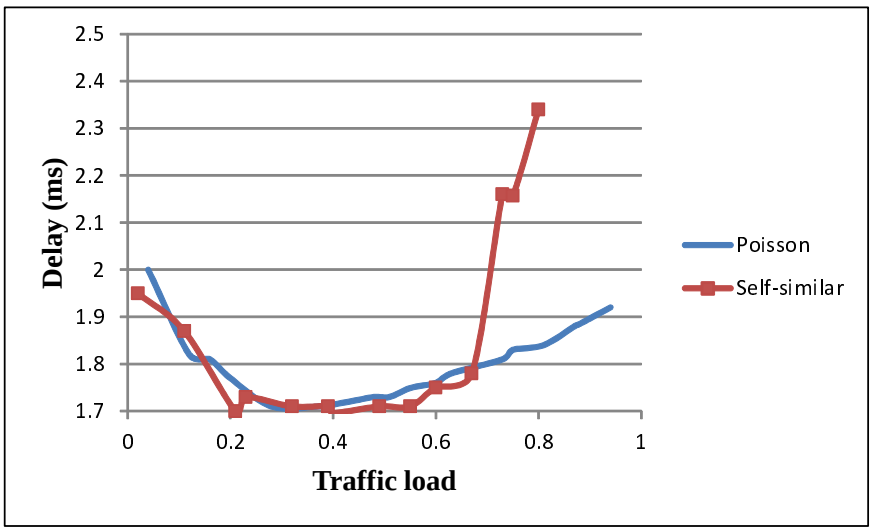

Figure 2.9 Delay vs. traffic load for Poisson and self-similar traffic.

performances with respect to traffic load for both Poisson and self-similar traffic is similar to numerical results of the Markov model for the Poisson traffic profile.

Figures 2.10 and 2.11 illustrate the impact of the number of listening cycles on the system performances. Similar to the theoretical analysis of the Poisson traffic, energy saving and delay performance decreases with the increase of the listening cycle durations.

Figure 2.12 and 2.13 show the impact of the number of the sleep cycles on the system performances for the Poisson and self-similar traffic. The results of this simulation is also similar to the numerical results of Poisson traffic, delay increases almost linearly with the increase of the sleep cycles since the "wait-to-wakeup" time dominates the overall packet delay, and energy saving increases with the increase of the sleep cycles, but is almost constant when the number of sleep cycles is increased to a certain number.

2.6 Summary

A simple sleep control scheme is proposed to efficiently put EPON ONUs into the sleep mode for energy saving. Downstream traffic scheduling rules at the OLT and sleep control rules at ONUs constitute two main parts of the proposed scheme. The sleep control scheme does not require modification of the EPON MAC protocol. It also eliminates the need of the handshake process and allows dynamic downstream bandwidth allocation. Therefore, it achieves high efficiency in both energy saving and bandwidth utilization. Performances of

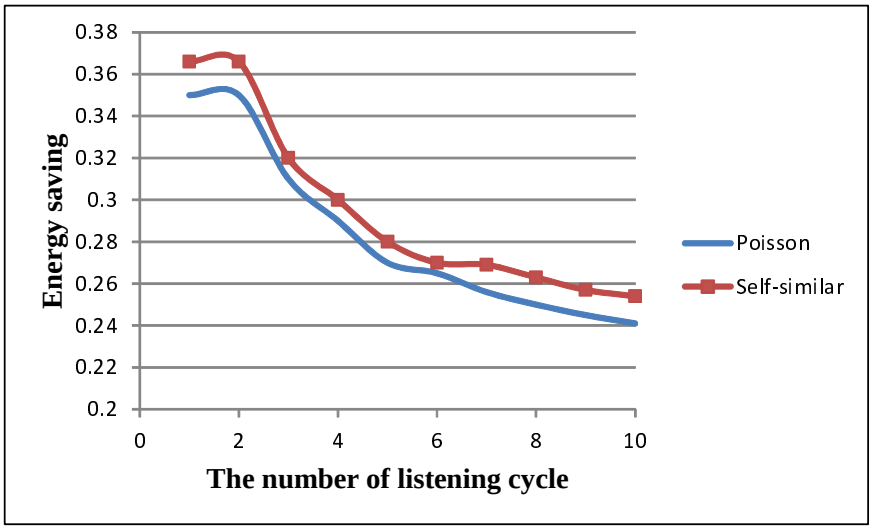

Figure 2.10 Energy saving vs. the number of listening cycles for for Poisson and self-similar traffic.

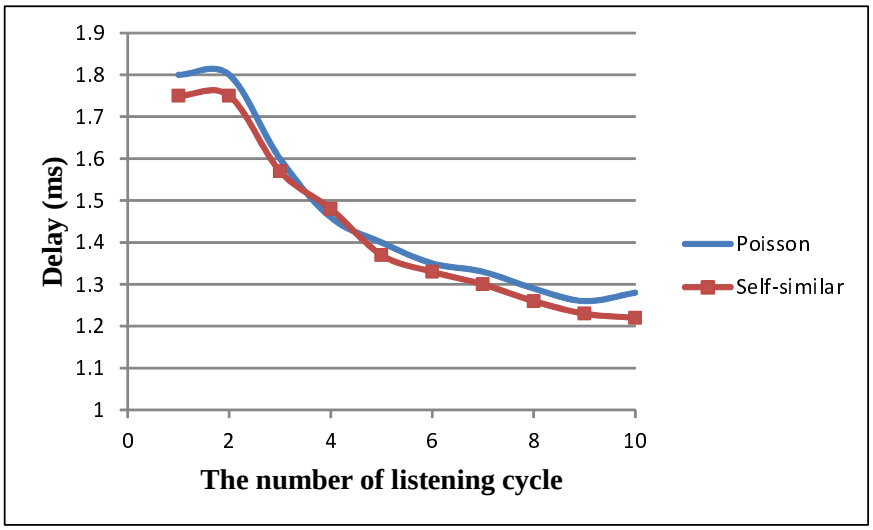

Figure 2.11 Delay vs. the number of listening cycles for Poisson and self-similar traffic.

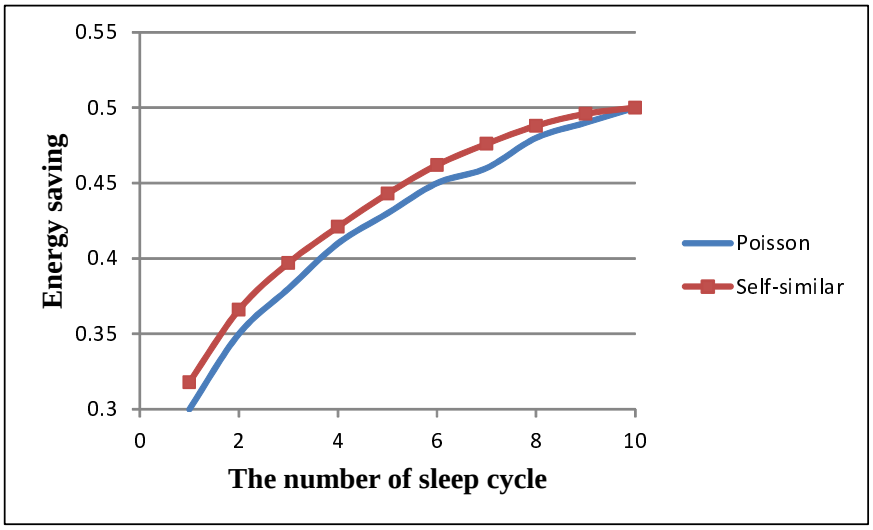

Figure 2.12 Energy saving vs. the number of sleep cycles for Poisson and self-similar traffic.

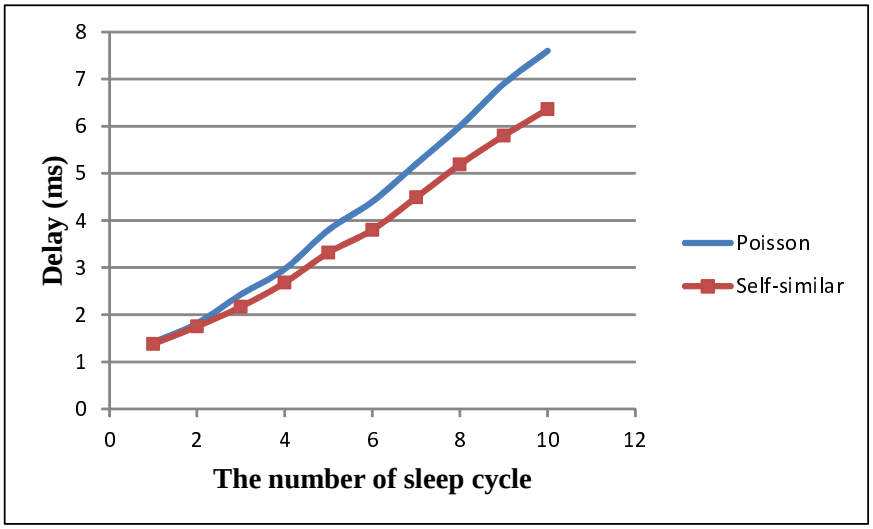

Figure 2.13 Delay vs. the number of sleep cycles for Poisson and self-similar traffic.

the proposed scheme is theoretically analyzed by employing semi-Markov chains. The energy saving and delay performances of our proposal scheme are demonstrated and evaluated by changing the sleep control parameters. It is illustrated that as large as 55% energy saving can be achieved when the network is lightly loaded.

CHAPTER 3

MULTI-POWER-LEVEL ENERGY SAVING MANAGEMENT

Multi-power mode devices are able to reduce the energy consumption of the network by disabling certain functions [20]. The EPON system adopts a TDM (Time Division Multiplex) mechanism to multiplex traffic onto a single wavelength in both upstream and downstream directions [37]. In order to avoid service degradation in EPON, proper design of a MAC-layer control and scheduling scheme is required. Putting ONUs in the sleep mode during the idle time has been widely proposed in the literature.

Yan *et al.* [54] proposed two scheduling algorithms to save the energy in EPON. In the first algorithm, upstream centric scheduling, the OLT buffers and sends the downstream traffic to a specific ONU during the pre-scheduled time for the ONU upstream traffic. In the second scheme, which is called downstream centric scheme (DCS), the proper time slots are scheduled for both upstream and downstream traffic. This scheme is suitable for delay sensitive applications with lower energy saving. The proposed management mechanism can save 10% energy as compared to the base model with no energy saving management.

Kubo *et al.* [29] proposed a sleep control scheme by using adaptive link rate (ALR) control functions to reduce the ONU active time and extend the sleep periods. In the proposed sleep and periodic wake up (SPW) operation, using three way handshakes, an ONU goes to the sleep mode. The sleeping ONU wakes up periodically to check if it has any upstream or downstream traffic to send or receive, respectively. According to the monitored traffic, the proper optical link rate is set in the multirate ONU.

In the majority of sleep control schemes, two power consumption levels are defined for an ONU. Low power consumption is defined during the sleep state in which the whole ONU goes to sleep to save the energy. High power consumption is defined in the active state in which all the sub systems of the ONU are completely functional.

Zhang and Ansari [57] proposed to put different components to sleep under different conditions and to form a multi-power-level ONU. They did not describe state transitions between all power levels, and left some rooms for future investigations.

Modeling each ONU data transmission with an M/G/1 queue with vacation, Dhaini *et al.* [17] computed the maximum ONU sleep time without proposing any sleep control scheme. However, they did not consider the downstream data transmission which can interrupt the ONU sleep time.

3.1 Contributions and Overview

In this Chapter, an efficient sleep control scheme is proposed to put the ONU in different levels of energy consumption depending on both the downstream and upstream traffic situations, and thus as much as 60% of the ONU energy can be saved. The trade-off between energy saving and traffic quality of service (QoS) in the simulation results is investigated. The proposed scheme is completely compatible with the MPCP control protocol and EPON standards (IEEE 802.3ah and IEEE 802.3av).

The IEEE 1904.1 standard also describes the system-level requirements needed to ensure service-level, multi-vendor interoperability of Ethernet Passive Optical Network (EPON) equipment. This standard is on top of IEEE 802.3 and IEEE 802.1, and complements them to ensure the interoperability at the physical layer and data link layer. Since the proposed algorithm is based on the mutual inference at the OLT and the ONU, it is completely compatible with the IEEE 1904.1 standard.

The rest of the chapter is organized as follows. Section 3.2 details the proposed sleep control scheme. Section 3.3 describes the traffic scheduling algorithm. The ONU transmitter is analytically modeled, and the duration of the transmitter sleep time is calculated in Section 3.4. Numerical and simulation results are presented in Section 3.5. Section 3.6 summarize the chapter.

3.2 Sleep Control Scheme

Two optical devices that consume the most energy in the ONU module are the optical receiver (Rx) and the optical transmitter (Tx). The ONU transmitter block consists of laser and driver, and the ONU receiver block consists of the photo detector, front-end circuit, and back end circuit [49]. Owing to the burstiness of upstream and downstream traffic of the ONU, putting Rx and Tx in the sleep mode when no traffic is observed can save a significant amount of ONU energy. In some applications, e.g., file downloading, ONU has

only downstream traffic. In this case, the Tx, which does not perform any task, can go to the sleep mode [59]. Similarly, during the upstream transmission only, the ONU can disable the functionality of its receiver. Frequent changes of the ONU state from the active mode to the sleep mode and vice versa waste a considerable amount of energy. This overhead is the time taken for the ONU to re-synchronize to the central office (CO) clock after waking up from the sleep mode. In order to avoid frequent changes of the states, and owing to the burstiness of the arrival traffic, it is more efficient for the ONU to spend some time in the listening mode before putting each component to the sleep mode. Therefore, the ONU can immediately return to the active state upon receiving a packet.

3.2.1 Multi-level Power Consumption

In the proposed energy saving model, there are 9 states (modes) that the ONU can enter in different situations. The ONU energy cosumption in each state is different. Figure 3.1 illustrates the level of power consumption of each state. TA, TL, and TS represent the active, listening, and sleep mode of the ONU transmitter, respectively. Likewise, RA, RL, and RS indicate the active, listening, and sleep mode of the ONU receiver, respectively. The ONU receiver typically consumes low power in the active mode [51]. Therefore, the ONU in the RL/TA and RS/TA states still consume a large amount of energy as the transmitter is active. In the RL state, the ONU receiver is still active, but it does not receive any traffic. Thus, the power consumption is slightly lower than the active state. The ONU transmitter consumes the most portion of the ONU power [49]. Therefore, transmitter sleep control plays a key role in reducing the ONU power consumption.

To elicit the model architecture and the sleep control mechanism, two different Markov models for the ONU transmitter and the receiver are considered. The ONU can thus assume six states: “Rx Awake”, “Rx Listen”, “Rx Sleep”, “Tx Awake”,“Tx Listen”, and “Tx Sleep” as shown in Figure 3.2.

In the “Rx Awake” and “Tx Awake” states, the ONU receiver and transmitter are fully functional, respectively. The ONU stays for a specific amount of time in the “Rx Listen” state before being transferred to the “Rx Sleep” state. During the “Rx Sleep” state, the ONU receiver is in the low power mode and cannot receive any traffic. “Tx Listen”

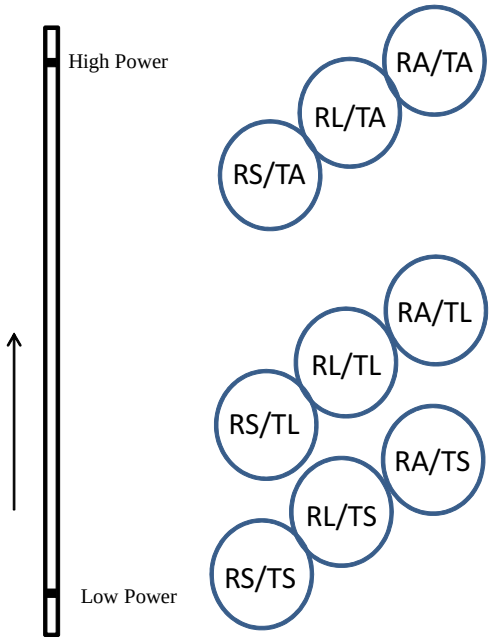

Figure 3.1 ONU multi-level power consumption.

represents the state in which the ONU transmitter is in the active mode, but it does not transmit any traffic. Since all the functions are working in the listening states, the power consumption of the ONU in this state is higher than the "Tx Sleep" state. When the ONU is in the "Tx Sleep" state, all the transmitter functions are powered off while the receiver functions depend on the receiver status. The ONU is powered off completely whenever both transmitter and receiver are in the "Tx Sleep" and "Rx Sleep" states, respectively, in which case the ONU consumes the least amount of power.

3.2.2 Sleep Control and ONU State Transition

The proposed sleep control scheme is based on the mutual inference between the OLT and the ONU. During the time that the receiver is in the "Rx Awake" state and the transmitter is in the "Tx Awake" state, the ONU receives downstream packets and transmits upstream packets at the same time. Transition from the "Rx Awake" state to the "Rx Listen" state, and transition from the "Rx Listen" state to the "Rx Sleep" state are defined in Rule 1 and Rule 2, respectively.

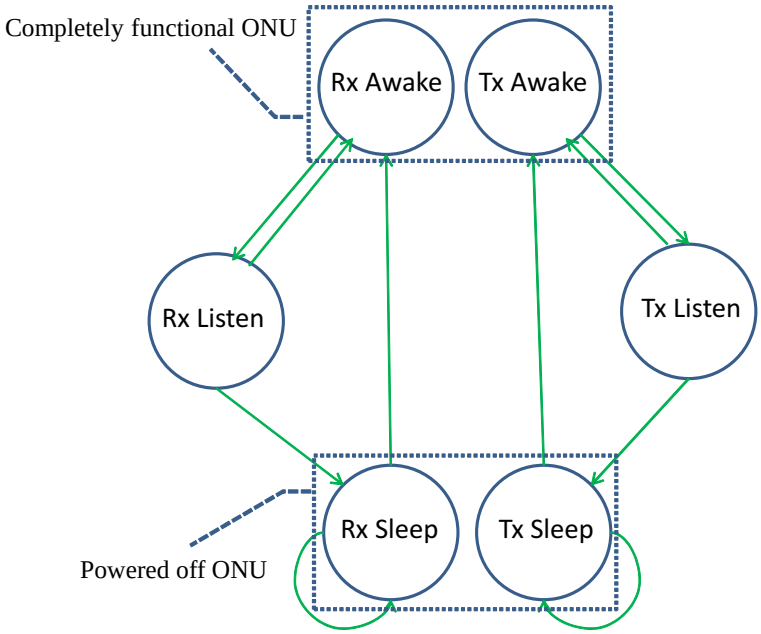

Figure 3.2 ONU state transition.

Rule 1. *If the ONU does not receive any packets within the current traffic scheduling cycle, the ONU infers that the downstream queue is empty, and the receiver enters the "Rx Listen" state.*

The OLT is aware of this transition, but the functionality of a listening ONU is the same as an active receiver from the OLT point of view. Whenever the OLT receives the traffic destined to a listening ONU, it sends the traffic immediately. By receiving any packets from the OLT side, a listening receiver changes its state to active.

Rule 2. *If the OLT does not assign any traffic to the ONU during the pre-determined listening cycles, the ONU receiver enters the "Rx Sleep" state and spends a pre-determined period of time in the sleep state.*

Since the OLT did not allocate any traffic to the ONU in the receiver listening period, it infers that the ONU enters the sleep mode. Time duration of "Rx Listen" and "Rx Sleep" of the ONU are predefined and known for the two parties.

For the period of the "Rx Sleep" time, the OLT buffers the traffic destined to an asleep ONU. After the completion of the sleep period, the OLT starts sending the buffered traffic to the ONU and the ONU receiver state is changed to active. If no traffic has been buffered

for the sleep ONU, the ONU skips the listening state, and returns to the "Rx Sleep" state. Since the OLT knows the duration of the sleep and listen states, it infers the states of the ONU, thus eliminating the necessity of handshake messages.

Transitions between listening and sleep states of the ONU transmitter are the same as the ONU receiver. Transition from the "Tx Awake" state to the "Tx Listen" state, and transition from the "Tx Listen" state to the "Tx Sleep" state are defined in Rule 3 and Rule 4, respectively.

Rule 3. *If the ONU does not have any traffic from the user side to send, it enters the "Tx Listen" state.*

Since the ONU bandwidth request is zero, the OLT infers that the upstream queue is empty, and is aware of the ONU change of the state. During the ONU listening time, whenever the ONU receives the traffic from the user side, it requests the proper bandwidth and changes its current state to the active state.

Rule 4. *If the ONU does not receive any traffic from the user side for the pre-determined transmitter listening period, the ONU transmitter goes to the "Tx Sleep" state.*

Since the ONU transmitter can be triggered by the incoming packets from the users, the time duration of the ONU sleep transmitter varies in each "Tx Sleep" state. Each incoming packet can tolerate a specific amount of time in the queue before being sent. Depending on the packet class of service, packets can be buffered in the transmitter for a limited time, and transmitter in the sleep mode can sleep for a longer time. The calculation of the ONU transmitter time will be discussed in Section 3.4.

The minimum energy consumption is during the time when both the ONU transmitter and receiver are in their sleep states. In [59], the semi-Markov chain model is used to describe the operation of the ONU receiver. The delay and energy saving performance of the ONU in the situation of just having downstream traffic was analyzed in Chapter 2. Since the Markov model for the transmitter and the receiver are equivalent, in the following section, the discussion is more about the traffic scheduling of the ONU in the existence of bidirectional traffic .

3.3 Traffic Scheduling Algorithm

Different settings of the listening time duration and sleep time duration, which are defined in terms of multiples of the traffic scheduling cycle (T_{cycle}), affect the energy saving efficiency. The traffic scheduling cycle is assumed to be fixed ($2ms$). From now, it is referred to the number of cycles that the ONU transmitter or receiver stays in the sleep state as sleep cycles, and the number of cycles that the ONU transmitter or receiver stays in the listening state as listening cycles. As discussed earlier, the OLT knows all the information of the sleep control scheme implemented at each ONU which includes the listening time duration and sleep time duration. Whenever the OLT does not allocate any traffic to a specific ONU for a duration of the ONU's listening time, it infers that the ONU receiver is in the "Rx Sleep" state. Since the OLT is also aware of the ONU receiver sleep time, it buffers the arrival downstream traffic of the sleeping ONU until the ONU wakes up.

In the upstream direction, the ONU buffers arrival upstream traffic during the transmitter sleep time. When the transmitter wakes up, the ONU sends its bandwidth request for the next scheduling cycle to the OLT. The OLT receives the requests from all the ONUs, and assigns the bandwidth for each ONU based on dynamic bandwidth allocation (DBA). At the beginning of the scheduling cycle, the OLT sends the grant message, which contains the start transmission time and duration of the transmission (assigned bandwidth to the ONU), to each ONU.

In the situation that the ONU receiver is in the sleep state while the transmitter is working, the ONU needs to receive the grant message for upstream data transmission. Algorithm 1 describes the traffic scheduling in the case that the ONU receiver is in the sleep mode and the ONU transmitter is in the active mode. "FBA bandwidth" is the bandwidth that is calculated by the fixed bandwidth allocation (FBA) scheme which grants each ONU with a fixed time slot length. When the ONU reciever is in the sleep mode, the ONU requests the minimum bandwidth between "FBA bandwidth" (BW_{FBA}) and its required bandwidth (BW_r). The OLT is aware of the ONU receiver state and assigns the exact requested bandwidth to the ONU during the receiver sleep time. In order to set the start time of the ONU transmission in the next cycle, while the ONU receiver is in the sleep state, the OLT and the ONU keep track of the previous ONU transmission start time (T_{ps}) and

T_{ps}: Previous granted start time for the ONU transmission;

T_S: Current granted start time for the ONU transmission;

Max_{cycle}: maximum number of traffic scheduling cycles;

Num_{cycle}: number of traffic scheduling cycle;

$Num_{cycle} = 0$;

while $Num_{cycle} < Max_{cycle}$ **do**

  if *Tx sleep* **then**

    $T_{ps} = T_{ps} + T_{cycle}$;

  end

  if *Rx Sleep* **then**

    if *Tx Active* **then**

      $RequestBW = min(BW_r, BW_{FBA})$;

      The OLT allocates $RequestBW$ to the ONU;

      $T_s = T_{ps} + T_{cycle}$;

      $T_{ps} = T_s$;

    end

  else

    OLT allocates the bandwidth based on DBA scheme;

    OLT sends the grant message including the assigned bandwidth and T_s;

  end

  $Num_{cycle} = Num_{cycle} + 1$;

end

Algorithm 1: Bandwidth allocation algorithm for the upstream traffic.

set $T_{ps} + T_{cycle}$ as the next start time (T_s). If the transmitter was in the sleep state and wakes up in the current state, the OLT and the ONU have to keep the information of the last start time. During the time that the ONU transmitter is in the "Tx Sleep" state, T_{ps} is incremented by the ONU transmitter sleep time.

3.4 Theoretical Analysis

In this section, the model with both Poisson upstream and downstream traffic is analyzed. Downstream and upstream packet arrival rates are assumed to follow the Poisson process with rate λ_D and λ_U, respectively. Service rate is also exponentially distributed in the downlink and uplink with the mean value of μ_D and μ_U, respectively.

The probability of having α downstream arrival packets at the OLT and departure packets from the OLT in a traffic scheduling cycle is obtained by Equations 3.1 and 3.2, respectively.

$$P^a_{DL}(\alpha) = e^{-\lambda_D T_{cycle}} \cdot (\lambda_D \cdot T_{cycle})^\alpha / \alpha! \tag{3.1}$$

$$P^d_{DL}(\alpha) = e^{-\mu_D T_{cycle}} \cdot (\mu_D \cdot T_{cycle})^\alpha / \alpha! \tag{3.2}$$

Similarly, in the upstream direction, the probability that α packets arrive at the ONU transmitter and depart from the ONU transmitter is obtained as follows.

$$P^a_{UL}(\alpha) = e^{-\lambda_U T_{cycle}} \cdot (\lambda_U \cdot T_{cycle})^\alpha / \alpha! \tag{3.3}$$

$$P^d_{UL}(\alpha) = e^{-\mu_U T_{cycle}} \cdot (\mu_U \cdot T_{cycle})^\alpha / \alpha! \tag{3.4}$$

When an asleep ONU wakes up, it needs to recover the OLT clock and to be synchronized with the network which imposes an overhead to the system. Wong *et al.* [51] proposed two ONU architectures which reduce the overhead time to tens of nanoseconds.

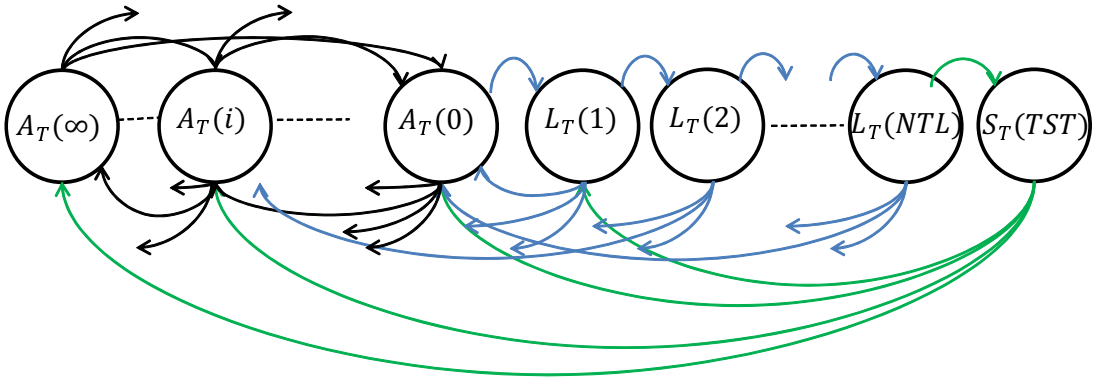

Figure 3.3 ONU transmitter Markov chain.

Considering these two architectures, this overhead time is negligible as compared to the duration of a traffic scheduling cycle.

The Markov chain model for the ONU transmitter and the ONU receiver assumes the following states:

- $A_{T(i)}$ and $A_{R(j)}$ are the "Awake" states in which i refers to the number of queued upstream packets, and j refers to the number of queued downstream packets.
- $L_{T(i)}$ and $L_{R(j)}$ are the "Tx Listen" and the "Rx Listen" states, respectively, where i (j) represents the number of cycles taken by the ONU transmitter (receiver) in the listening mode.
- $S_{T(i)}$ and $S_{R(j)}$ refer to the status that the ONU transmitter and receiver stay asleep, respectively, where i and j represent the number of sleep cycles for the ONU transmitter and receiver to be asleep, respectively.

State transitions are performed based on the rules discussed in Sec. 3.2.2. State transition between the active states depends on the number of arrival and departure packets in each cycle.

- Transition from $A_{R(r)}$ to $A_{R(k)}$ ($A_{T(r)}$ to $A_{T(k)}$) for $r > k$ happens when the number of departure packets are $r - k$ more than the number of arrival packets by the end of the traffic cycle.
- Transition from $A_{R(r)}$ to $A_{R(k)}$ ($A_{T(r)}$ to $A_{T(k)}$) for $r < k$ happens when the number of arrival packets are $r - k$ more than the number of departure packets by the end of the traffic cycle.
- If all the queued and arrival packets could be served in one cycle, transition to $A_{R(0)}$ state occurs.

The Markov chain model for the ONU transmitter is represented in Figure 3.3. The Markov model for the ONU receiver has been previously discussed in [59]. If no packet

arrives at the OLT in the next traffic scheduling cycle and the current state of the ONU receiver is $A_{R(0)}$, the ONU receiver state transits to $L_{R(1)}$; if the current state is $L_{R(k)}$, the ONU receiver state transits to $L_{R(k+1)}$. Transitions from $A_{T(0)}$ to $L_{T(1)}$ and $L_{T(k)}$ to $L_{T(k+1)}$ also occur in the same way for the ONU transmitter.

Consider the maximum number of listening cycles for the ONU transmitter (receiver) before going to the sleep state as NTL (NRL). Whenever the number of i (j) in $L_{T(i)}$ ($L_{R(j)}$) for the ONU transmitter (receiver) reaches NTL (NRL), transition from $L_{T(NTL)}$ to $S_{T(1)}$ ($L_{R(NRL)}$ to $S_{R(1)}$) occurs.

By the time that the ONU receiver goes to the sleep state, it does not wake up until the number of sleep cycles reaches the maximum defined amount (NRS). Depending on the number of downstream arrival packets during the sleep period, transition from $S_{R(NRS)}$ to any of the receiver active states $A_{R(0)}, A_{R(1)}, ...$ could happen. Upon waking up, if no traffic has arrived during the sleep time, the ONU receiver will sleep for another NRS cycles.

Since the duration of the ONU transmitter sleep time is not pre-defined, each ONU transmitter sleeps for a different amount of time. TST is defined as the ONU transmitter sleep time.

3.4.1 The ONU Transmitter Sleep Duration

Triggering the sleep ONU to wake up by arrival traffic can only be performed in the ONU transmitter side. Before the OLT sends the downstream traffic to the asleep ONU, the ONU receiver has to be waken up. Suppose that the quality of service in the downstream direction needs a handshake to wake up the ONU as the ONU receiver sleep time is no longer fixed. However, in the upstream direction, the ONU has to request the required amount of bandwidth to send the data in both algorithms (algorithm with predefined sleep cycles and algorithm with calculated sleep time based on QoS class of arrival packets). Since the proposed algorithm for the ONU receiver exhibits a trade-off between energy saving and traffic quality of service (QoS), considering the QoS for the upstream traffic is more reasonable. Therefore, the receiver sleep cycles are predefined while the ONU transmitter sleep time can be calculated by considering the quality of service (QoS) class of each arrival packet [17].

In the proposed sleep control scheme, the ONU receiver and transmitter stay active until no more packets remain in the queue. In the upstream transmission, M/G/1 queues are used for three different priority classes: the constant bit rate (CBR) queue has the highest priority, the variable bit rate (VBR) queue has the second highest, and the Best Effort (BE) queue has the lowest priority. All dedicated packets to each queue are from the same QoS category [2]. An acceptable delay threshold is defined for each category, implying that packet delay for each category cannot exceed the threshold.

The ONU transmitter goes to the sleep mode whenever it does not receive any traffic during specific traffic cycles (Tx Listening cycles). If it receives a packet from the user side during the mentioned interval, the ONU transmitter state will be changed to the active state. The ONU requests the bandwidth based on Algorithm 1 to send the received packets. However, during the ONU sleep time, received packets are buffered and will be transmitted later. Therefore, the queue model is M/G/1 with vacations. Parameters of the proposed model are denoted as follows:

N: Number of ONUs.

i : Queue index ($i = 0, 1, 2$).

j : ONU index ($j = 0, 1, 2, .., (N - 1)$).

$\lambda_{U(i,j)}$: Packet arrival rate of queue i at ONU j.

μ_U: Packet service rate.

v_j: The ONU j total vacation time.

$W_{i,j}$: The average waiting time of a packet from queue i at ONU j.

$T_{i,j}$: Total delay of a packet from queue i at ONU j.

$Delay_i$: Delay threshold of the packets from queue i.

$Sleep_{i,j}$: Sleep time of ONU j based on queue i.

$TxSleep_j$: Maximum transmitter sleep time of ONU j.

$T_{propagation,j}$: Propagation delay between OLT and ONU j.

Total delay of a packet consists of queuing delay, service time (transmission delay), and propagation delay. Average service time and second moment of service time of the packets from queue i are expressed as $X_i = 1/\mu$ and $E[X_i^2]$, respectively. Using the P-K formula [12],

following the method exploited in [17], the average waiting time for the packets belonging to queue i is obtained as follows.

$$W_{i,j} = \frac{\lambda_{i,j} E[X_i^2]}{2(1-\rho_j)\sum_{i=0}^{2} \lambda_{i,j}} + \frac{3v_j}{2} \tag{3.5}$$

where $\rho_j = \sum_{i=0}^{2} \rho_{i,j}$, and $\rho_{i,j} = \lambda_{i,j}/\mu$ is the utilization factor of queue i at ONU j.

Total delay of a packet in the system is equal to the following:

$$T_{i,j} = W_{i,j} + 1/\mu + T_{propagation,j} \tag{3.6}$$

Neglecting the overhead time, v_j is equal to the ONU transmitter sleep time. The ONU transmitter sleep time based on queue i depends on the delay threshold of the packets in the queue, and can be computed as:

$$Sleep_{i,j} = Delay_i - T_{i,j} - T_{cycle} \tag{3.7}$$

The time duration between waking up the ONU transmitter and sending the upstream traffic is approximately one traffic scheduling cycle. At first, the ONU has to send the bandwidth request to the OLT, and then receives the grant message in which the time of the ONU transmission is granted for the upcoming cycle.

The ONU transmitter is triggered whenever the delay threshold of one of the queues is about to be met. Therefore, the maximum transmitter sleep time is equal to :

$$TxSleep_j = min(Sleep_{0,j}, Sleep_{1,j}, Sleep_{2,j}) \tag{3.8}$$

In each traffic scheduling cycle that the OLT does not receive any traffic from an ONU, it counts the cycle as the first listening cycle. From this point, the OLT just assigns the amount of bandwidth for the ONU report message. Since the OLT is aware of the duration of the ONU transmitter listening state, it can infer the change of the state from listening to the sleep state. Whenever the OLT receives the report message including the bandwidth request, it infers the change of the state to active, assigns the bandwidth accordingly, and sends back the grant message.

3.5 Numerical and Simulation Results

Recent studies have focused on either upstream or downstream traffic to make a sleep decision for the ONU. Here, both upstream and downstream traffic are considered concurrently by enabling separate sleep modes for the ONU transmitter and receiver. The SPW operation also imposes too much overhead on the system as making a decision is based on three way hand shaking. Therefore, the results are compared with the base model. Both numerical and simulation results are conducted to validate the effectiveness of the proposed solution. The numerical results are conducted based on the mathematical equations of this work (Section IV) and the exploited steady state probabilities of the Markov model from [59]. In the numerical results, Poisson traffic arrival is considered for both upstream and downstream traffic which is independent from the distribution of the packet size. The packet size is assumed to be exponentially distributed. In the simulation results, self-similar traffic is used with the Hurst parameter of 0.8. Some of the evaluation results are compared for both traffic, and the rest of the performance evaluation is conducted for self-similar traffic. 20% of the total traffic belongs to the CBR traffic with a fixed packet size of 70 bytes. The rest is equally divided between VBR and BE traffic with variable packet sizes uniformly distributed between 64 bytes and 1518 bytes. A 10G EPON supporting 32 ONUs operates at $10Gb/s$ in the downstream direction, and $2.5Gb/s$ in the upstream direction. Since having a fixed traffic scheduling cycle does not violate the EPON standards, the traffic scheduling cycle duration is set as $2ms$.

Traffic scheduling in the upstream and downstream direction is executed as follows. If the total traffic related to all the ONUs is less than the EPON capacity ($10Gb/s$ in the downstream and $2.5Gb/s$ in the upstream direction), all the traffic is scheduled, and all the queues become empty; otherwise, bandwidth allocation proportional to the ONU's bandwidth request is performed. The buffer size is also assumed to be infinite.

The power consumptions of the ONU transmitter and receiver in the active and sleep status are adopted from [1]. The ONU power consumptions in the "Awake" and "Sleep" states are 3.85 W and 750 mW, respectively. Power consumption of the ONU when the receiver is asleep and the transmitter is active would be 2.5 W, while it decreases to 1.7 W when the receiver is active and the transmitter goes to sleep. As for the listening status,

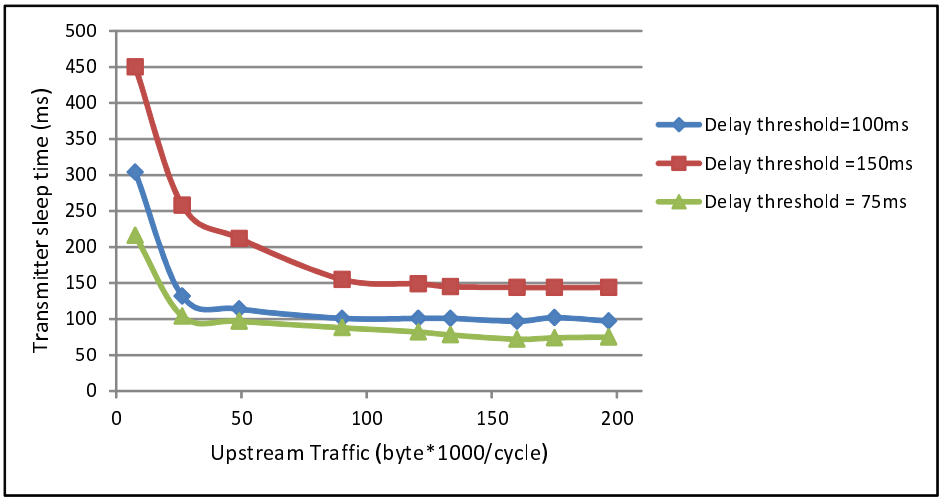

Figure 3.4 ONU transmitter sleep time for different delay thresholds (self-similar traffic).

the power consumption has to be within the range between the active and sleep power consumption. Since the exact number cannot be retrieved from publicly available literature, the simulations are performed using different values for the power consumption of the ONU receiver and transmitter in the listening status. Owing to the space constraint, the results are shown using 1.9 W for the "Tx listen" state when the receiver is active and 2.8 W for the "Rx listen" state when the transmitter is active, but the observations and conclusions can be similarly drawn for other values. Following Figure 3.1, energy consumptions of the other states are estimated using the mentioned numbers.

Three classes of service have different delay thresholds. Figures 3.4 and 3.5 show the direct impact of different delay thresholds on the duration of the ONU transmitter sleep time for self-similar and Poisson traffic, respectively. In each graph, the same delay threshold is set for three different classes. In the analytical results (Figure 3.5), the average transmitter sleep time cannot exceed the maximum threshold as it is calculated based on the average traffic arrival rate. However, during the low self-similar traffic load in the simulation result, the transmitter sleep time reaches the higher values when no traffic is observed. In the next simulation results, the delay threshold for CBR, VBR, and BE traffic is set as $100ms$, $1s$, and $50s$, respectively.

Figure 3.6 illustrates the system performance for different downstream traffic loads when the packet arrival is a Poisson process and the service time of each packet follows the exponential distribution. Here, the load is defined as the ratio between the total arrival

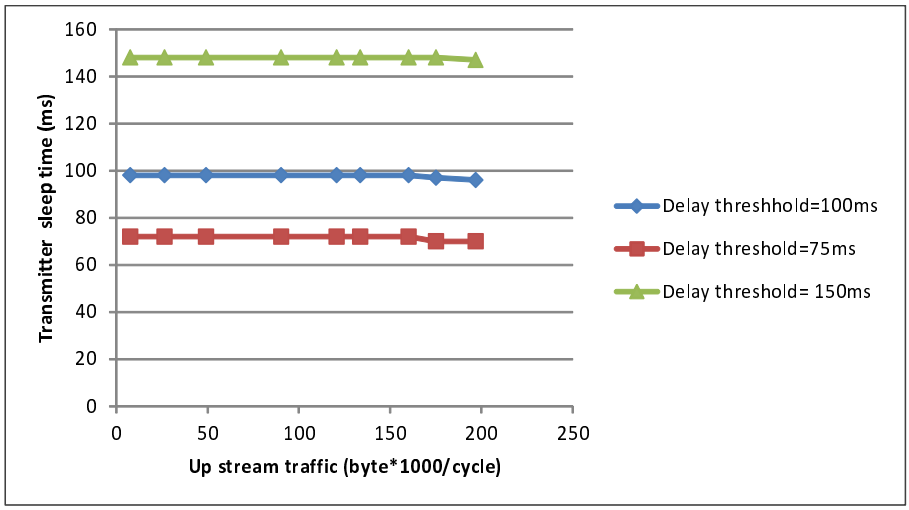

Figure 3.5 ONU transmitter sleep time for different delay thresholds (Poisson traffic).

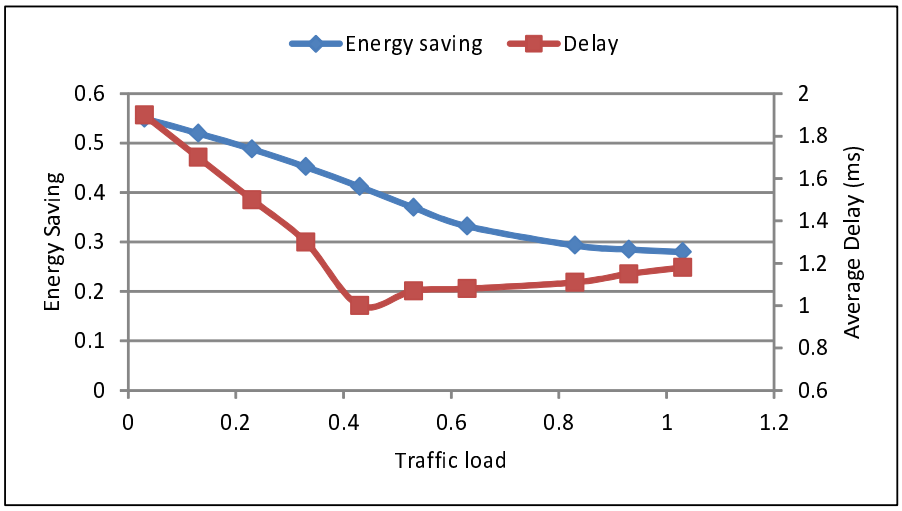

Figure 3.6 Energy saving and delay vs. downstream arrival traffic (numerical result).

traffic and the network capacity, and it increases from 0.03 to 1.03. The number of the Rx listening cycles, Rx sleep cycles, and Tx listening cycles are the same and equal to 2.

The primary axis (left y-axis) shows the energy saving trend as compared to the base model. Increasing the traffic load decreases the probability that the ONU stays idle in the listening cycles. Therefore, the probability of the ONU entering the sleep states to save energy decreases. The secondary axis (right y-axis) indicates the imposed delay for the downstream traffic. With a low traffic load, the queuing delay is negligible, but the time to wake up from the sleep state is dominant. Those packets which arrive when an ONU is sleeping have to wait until an ONU wakes up from the sleep state before being transmitted. By increasing the traffic load, as the probability that the ONU stays in the sleep state

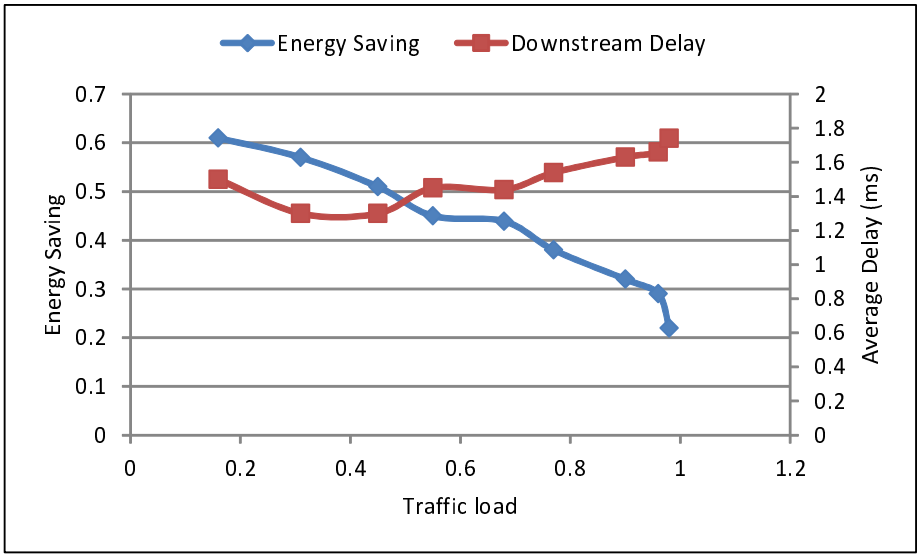

Figure 3.7 Energy saving and delay vs. downstream arrival traffic (simulation result).

decreases, the delay decreases. From a certain point, the queuing delay starts increasing, resulting in higher delay.

Figure 3.7 shows the system performances when the downstream traffic is self-similar. The numbers of listening cycles and sleep cycles are the same as those generated for the numerical results, and the traffic load varies from 0.16 to 0.98. It can be seen that the trend of both delay and energy saving performances with respect to the traffic load is similar to that of the numerical results for the Poisson traffic.

From the upstream point of view, the ONU transmitter sleeps for shorter time when the network is highly loaded. Figure 3.8 represents system performance in the upstream direction when the upstream and downstream follow self-similar traffic distribution. By increasing the load, the probability that the ONU transmitter goes to the sleep state decreases. Therefore, packets do not need to wait for the delay threshold to be met. The queuing delay is the dominant delay for upstream packets at high load.

The impact of changing the number of Rx listening cycles on the system performance is shown in Figure 3.9 (numerical result) and Figure 3.10 (simulation result). The number of Rx sleep cycles in both evaluations is equal to 2. As discussed in Section 3.2, the ONU receiver consumes a small portion of the ONU power consumption. Therefore, as depicted in Figure 3.9 and Figure 3.10, changing the receiver parameters has slight effects on energy

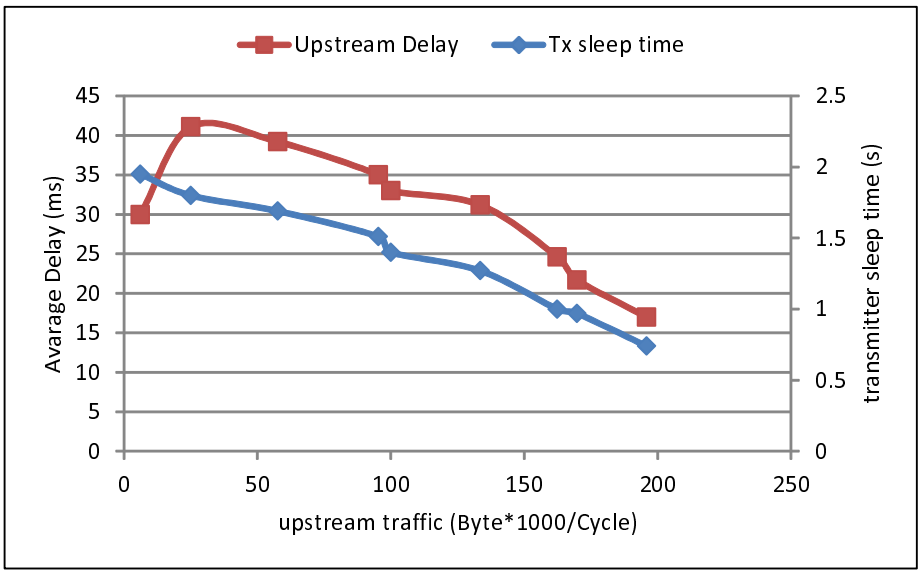

Figure 3.8 Transmitter sleep time and upstream delay vs. upstream arrival traffic (simulation result).

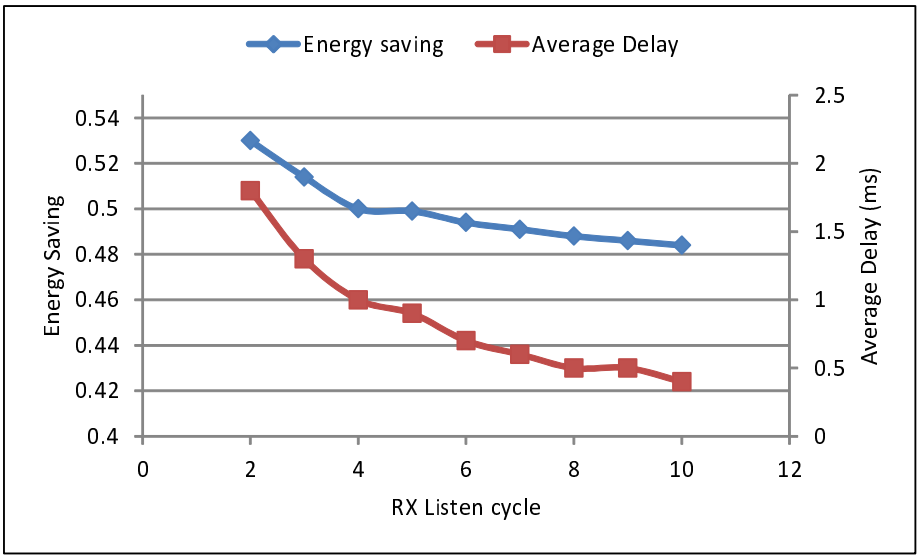

Figure 3.9 Energy saving and downstream delay performance vs. the number of Rx listening cycles (numerical result).

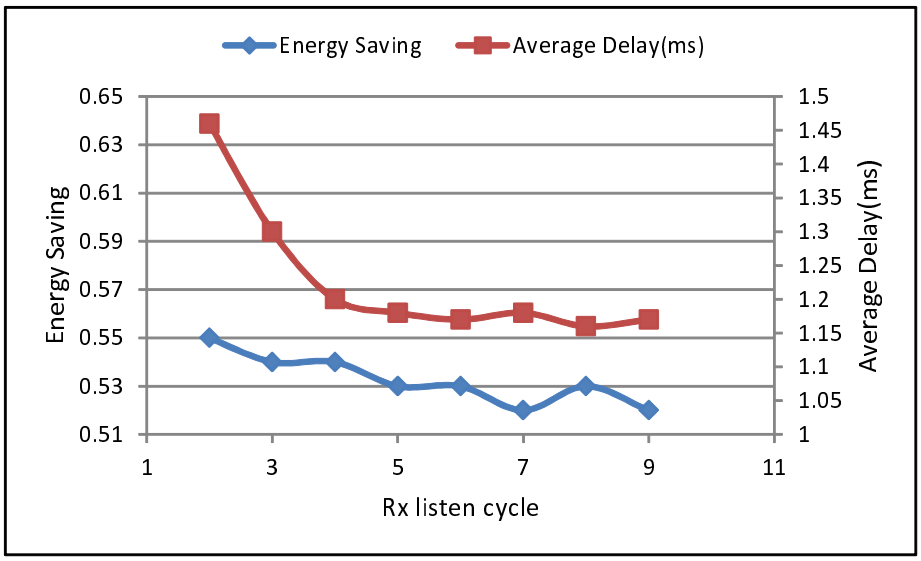

Figure 3.10 Energy saving and downstream delay performance vs. the number of Rx listening cycles (simulation result).

saving. Increasing the number of listening cycles increases the steady state probability of being in the listening state and decreases the steady state probability of being in the sleep state. When the probability that the ONU receiver stays in the sleep state decreases, the number of backlogged packets is small and they will be transmitted in a shorter time duration. Therefore, with the increase of the number of listening cycles, the steady state probability of being in the active state also decreases, and thus increases the energy saving.

As previously discussed, if the packets arrive when the ONU stays in the sleep state, they need to wait for the ONU to wake up. Increasing the number of Rx listening cycles decreases the probability that the ONU goes to the sleep state, and thus the downstream traffic is subject to lesser delay.

Increasing the number of Rx sleep cycles (Figure 3.11 and Figure 3.12) results in spending more time in the low power consumption mode, thus increasing the energy saving. The energy saving is almost constant when the number of sleep cycles increases beyond a certain number. Since the receiver stays idle for a longer time, the number of backlogged packets increases and the longer time duration is needed for the backlogged packets to be transmitted. Therefore, after a certain point, the steady state probability of being in the sleep state decreases. However, in Figure 3.12, energy saving shows an increasing trend,

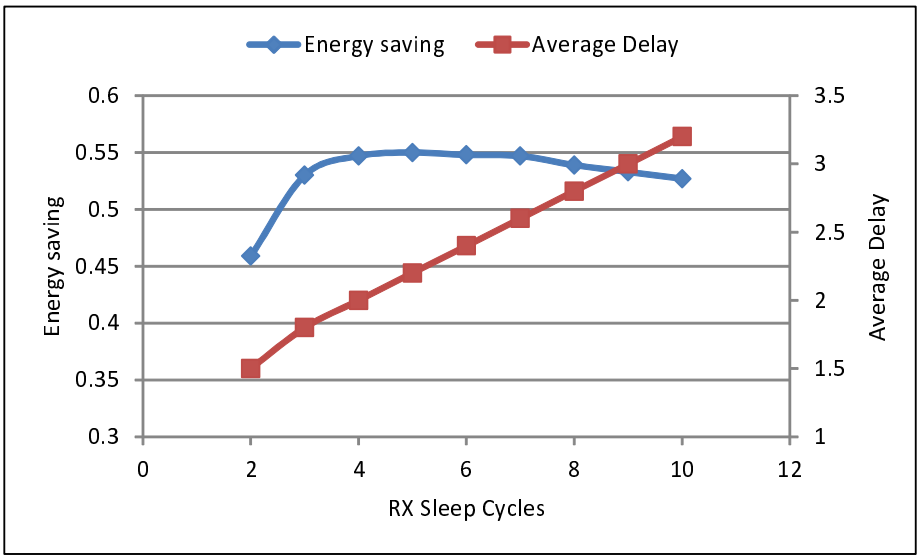

Figure 3.11 Energy saving and downstream delay performance vs. the number of Rx sleep cycles (numerical result).

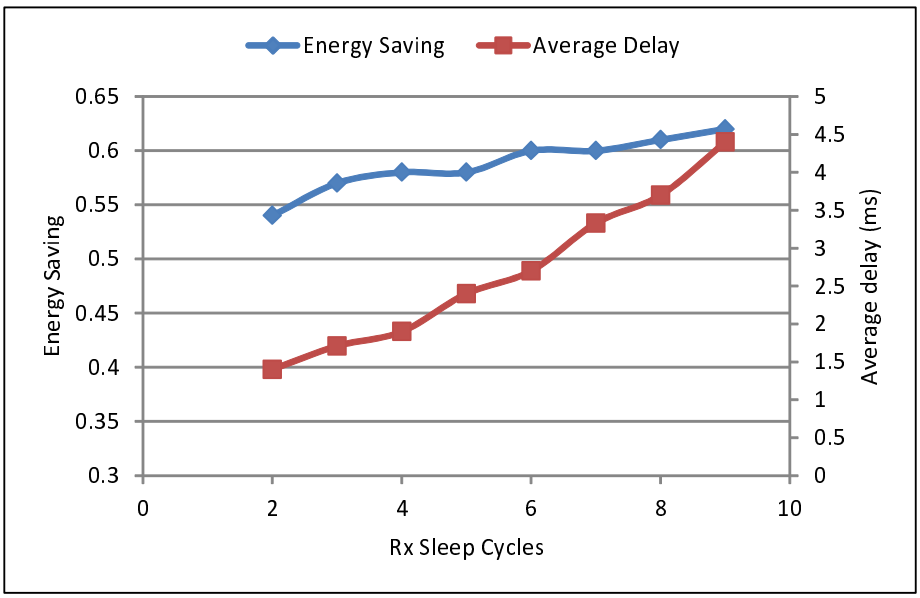

Figure 3.12 Energy saving and downstream delay performance vs. the number of Rx sleep cycles (simulation result).

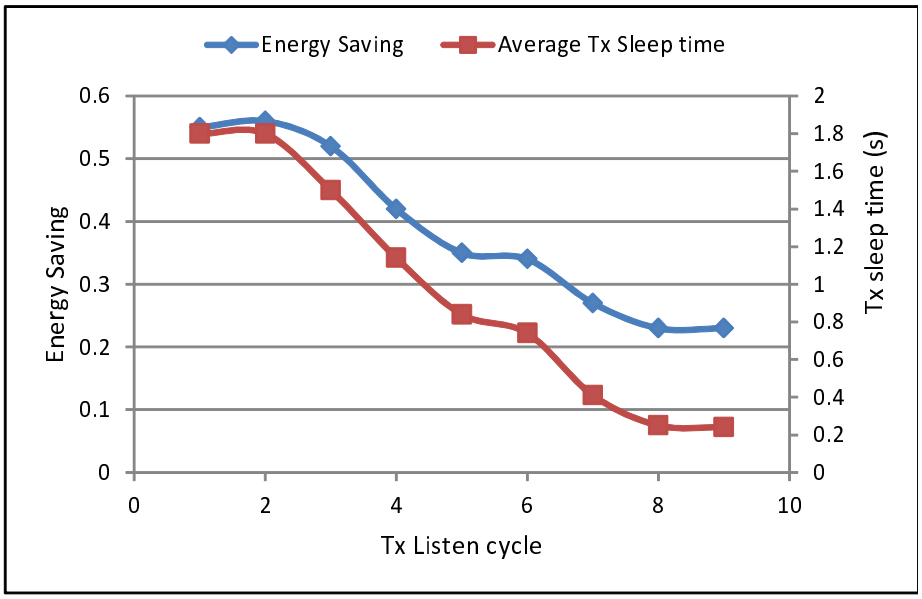

Figure 3.13 Transmitter sleep time and upstream delay vs. the number of Tx listening cycles (simulation result).

implying that the burstiness of the self-similar traffic affects the steady state probabilities of the active, listen, and sleep states. As it can be seen in both figures, delay is increasing linearly with the increase of the sleep time. This is because the dominant delay is the time that packets have to wait for the ONU to wake up from the sleep state. The number of Rx listening cycles is set as 2 in both numerical and simulation results.

Considering the number of Rx sleep cycles as 2 and the number of Rx listening cycle as 1, the confidence interval of the energy saving equals to $0.548 \pm (8.9 \times 10^{-3})$ for the given confidence level of 95%.

Changes of the ONU transmitter sleep time by increasing the number of Tx listening cycles is shown in Figure 3.13 for self-similar traffic. Increasing the number of listening cycles decreases the probability of keeping the ONU in the "Rx listen" state, decreases the probability of being in the sleep state, and increases the probability of the transmitter being active. Thus, the ONU transmitter sleep time and upstream delay both decrease by increasing the listening cycles.

3.6 Summary

A sleep control scheme is proposed for ONUs equipped with multi-level power consumption. Downstream traffic specifies the state of the ONU receiver, and the ONU transmitter acts according to the upstream traffic. In this chapter, the problem of putting the ONU receiver in the sleep state while the transmitter is still active is addressed. Whenever the upstream or the downstream traffic is not observed for a specific period of time, the ONU transmitter or receiver switches to the sleep mode, respectively. According to the upstream and downstream traffic arrival, the ONU decides whether to keep the transmitter and/or the receiver in the sleep mode. The proposed simple sleep control scheme and traffic scheduling algorithm are completely compatible with the EPON MAC protocol. Elimination of the handshake process also makes the sleep control scheme more efficient. Simulation results have validated the effectiveness of the proposed algorithm by saving up to 60% of the ONU energy during light traffic.

CHAPTER 4

DESIGN AND ANALYSIS OF GREEN OPTICAL LINE TERMINAL

In PONs, energy is consumed by optical line terminal (OLT) and optical network units (ONUs). Owing to the large quantity, ONUs consume a large portion of the overall PON energy [57]. Although OLT consumes a less amount of power than the total aggregated ONUs, one OLT line card does consume a much larger amount of power than one ONU. Reducing energy consumption of OLT is as important as reducing energy consumption of ONUs especially from the operators' and home users' perspectives. For the network operators, decreasing the energy consumption of OLT can significantly reduce the energy consumption of the central office, while decreasing the energy consumption of ONUs has small and likely negligible impacts on that of home users who have many other electrical appliances with much higher energy consumption.

The evaluation on energy efficiency of network capacity upgrading provide benchmarks both theoretically and practically on future high capacity network evolution. The concept of designing capacity-adaptive access networks is innovative and challenging, and introduces new requirements of capacity adaptive on the design of access networks as opposed to simply provisioning high data rate and high capacity as the primary design goal in the current practice.

Formerly, sleep mode and adaptive line rate have been proposed to efficiently reduce the power consumption of ONUs by taking advantages of the bursty nature of the traffic at the user side [29, 51, 15, 45]. It is, however, challenging to introduce "sleep" mode into OLT to reduce its energy consumption for the following reasons. In PONs, OLT serves as the central access node which controls the network resource access of ONUs. Putting OLT into sleep can easily result in service disruption of ONUs in communicating with the OLT. Thus, a proper scheme is needed to reduce the energy consumption of OLT without degrading services of end users.

4.1 Contributions

In this chapter, a novel energy-efficient OLT structure is proposed which can adapt its power-on OLT line cards according to the real-time arrival traffic. To avoid service degradation during the process of powering on/off OLT line cards, proper devices are added into the legacy OLT chassis to facilitate all ONUs communicate with power-on line cards.

The rest of the chapter is organized as follows. Section 4.2 presents the energy-efficient design of the OLT. Section 4.3 describes the use of optical switch to dynamically configure the communications between the OLT line cards and ONUs. The specification of the optical switches are detailed in Section 4.4. The OLT chassis is analytically modeled, and the performance of the system is analyzed in Section 4.5. The use of opto-mechanical and electrical switches in the OLT chassis is proposed in Section 4.6 and 4.7, respectively. Numerical and simulation results are presented in Section 4.8. Section 4.9 summarize the chapter.

4.2 Framework of the Energy-efficient OLT Design

In the central office, one OLT chassis typically comprises multiple OLT line cards that transmit downstream signals and receive upstream signals at different wavelengths. Each line card communicates with a number of ONUs. Two wavelengths for the uplink and the downlink are assigned to each ONU. In the currently deployed EPON and GPON systems, one OLT line card usually communicates with either 16 or 32 ONUs and such an arrangement is referred to as a PON segment. To avoid service disruptions of ONUs connected to the central office, all these OLT line cards in the OLT chassis are usually power-on all the time. To reduce the energy consumption of OLT, our main idea is to adapt the number of power-on OLT line cards in the OLT chassis to the real-time incoming traffic.

There are two types of subscribers that each network serves, business subscribers and residential subscribers. Business and residential areas are usually disjunct. It is more likely that each PON segment serves either business customers or residential customers. These two types of customers have different traffic profiles. Business users demand high bandwidth during the day and low bandwidth at night while residential customers request high bandwidth in the evening and low bandwidth during the day.

During the daytime, residential segments are lightly loaded. Therefore, one OLT line card can serve several residential segments. In the similar way, the traffic from the business segments can e combined to traverse a smaller number of line cards in the evening.

Business and residential segments usually have low bandwidth demands during the midnight. In these situations, the whole network is lightly loaded. In order to save energy, the number of line cards can be reduced based on the traffic volume.

Parameters of the proposed model are notated below:

C_u: Data rate of one OLT line card in the upstream direction.

C_d: Data rate of one OLT line card in the downstream direction.

L: Total number of line cards (PON segments).

N_j: Number of ONUs connected to PON segment j.

T: Fixed traffic cycle in TDM PON.

$u_{i,j}(t)$: Arrival upstream traffic rate from ONU i of PON segment j at time t.

$d_{i,j}(t)$: Arrival downstream traffic rate to ONU i of PON segment j at time t.

$l(t)$: smallest number of required OLT line cards at time t.

By powering on all the OLT line cards, the overall upstream data rate and downstream data rate accommodated by the OLT chassis equal to $C_u \cdot L$ and $C_d \cdot L$, respectively. $C_u \cdot L$ (or $C_d \cdot L$) may be greater than the real-time upstream (or downstream) traffic.

The traffic rate of each segment cannot be more than the provisioned capacity of the dedicated fiber. Therefore, the following constraints have to be satisfied for any segment j:

$$\sum_{i=1}^{N_j} u_{i,j}(t) \leq C_u$$
$$\sum_{i=1}^{N_j} d_{i,j}(t) \leq C_d \tag{4.1}$$

The real time upstream and downstream traffics are defined as $\sum_{j=1}^{L}\sum_{i=1}^{N_j} u_{i,j}(t)$ and $\sum_{j=1}^{L}\sum_{i=1}^{N_j} d_{i,j}(t)$, respectively. Then,

$$l(t) = max(\lceil \sum_{j=1}^{L}\sum_{i=1}^{N_j} u_{i,j}(t)/C_u \rceil, \lceil \sum_{j=1}^{L}\sum_{i=1}^{N_j} d_{i,j}(t)/C_d \rceil) \tag{4.2}$$

The ultimate objective is to **power on only $l(t)$ OLT line cards to serve all N ONUs** at a given time t instead of powering on all L line cards. However, powering off

OLT line cards may result in service disruptions of ONUs communicating with these OLT line cards. To avoid service disruption, power-on OLT line cards should be able to provision bandwidth to all ONUs connected to the OLT chassis. To address this issue, we propose several modifications over the legacy OLT chassis to realize the dynamic configuration of OLT as will be presented next.

4.3 OLT with Optical Switch

To dynamically configure the communications between OLT line cards and ONUs, one scheme we propose is to place an optical switch in front of all OLT line cards as shown in Figure 4.1 (a). The function of the optical switch is to dynamically configure the connections between OLT line cards and ONUs. When the network is heavily loaded, the switches can be configured such that each PON system communicates with one OLT line card.

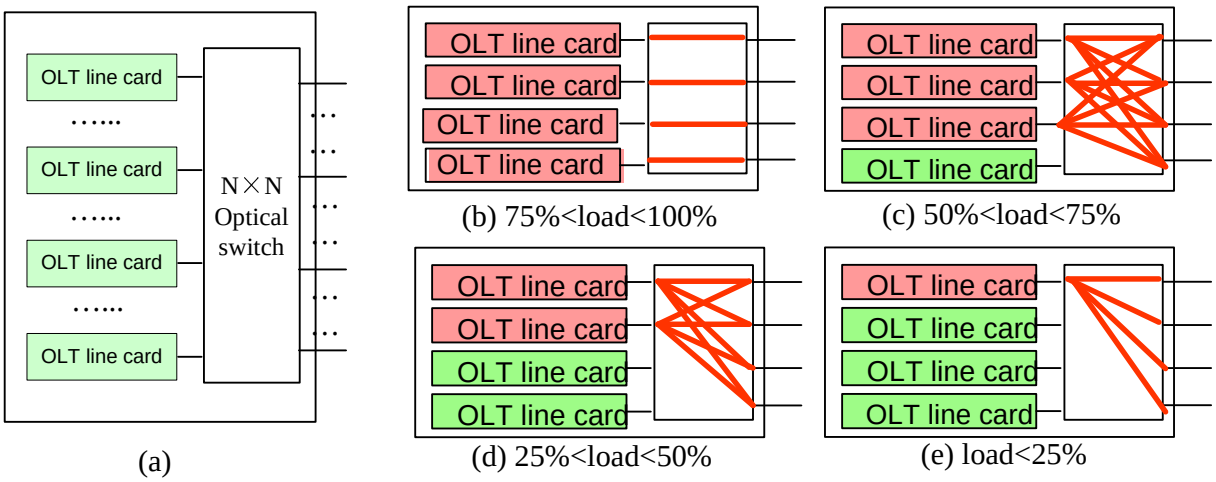

Figure 4.1 OLT with optical switches.

As discussed in Section 4.2, when the network is lightly loaded, the switches can be configured such that multiple PON systems communicate with one line card. Then, some OLT line cards can be powered off, thus reducing energy consumption.

Assume the energy consumption of the optical switch is negligible. As compared to the scheme of always powering on all L line cards, the scheme of powering on only $l(t)$ line cards at time t can achieve relative energy saving as large as

$$1 - \frac{l(t)}{L} \tag{4.3}$$

Then, the average energy saving over time span T equals to

$$\frac{1}{T}\int_{t=0}^{T}(1-\frac{l(t)}{L})dt \tag{4.4}$$

We define the traffic load as the maximum of upstream and downstream traffic loads to determine the required number of line cards:

$$load = max(\sum_{j=1}^{L}\sum_{i=1}^{N_j} u_{i,j}(t)/C_u L \ , \ \sum_{j=1}^{L}\sum_{i=1}^{N_j} d_{i,j}(t)/C_d L)$$

The process of changing the switch configuration is time consuming, and frequent change of each line card's status may degrade the ONU performance. Since the traffic of the ONUs is also bursty and changes dynamically, it is more efficient to monitor the traffic for an observation period (T_O) before changing the switch configuration.

If the traffic load of the network remains below a threshold for T_O, the number of line cards will be adjusted accordingly. By dynamically configuring switches, the number of power-on OLT line cards is reduced from L to x when the traffic load falls between $(x-1)/L$ and x/L for a period of T_O. Thus, a significant amount of power can be potentially saved.

Figure 4.1 (b)-(e) illustrates the configurations of a switch for the case that one OLT chassis contains four OLT line cards. The number of power-on OLT line cards is reduced from four to three, two, and one when the traffic load falls within the range $[50\%, 75\%]$, $[25\%, 50\%]$, and $[0, 25\%]$, respectively.

By equipping the OLT chassis with proper optical switches, the communications between OLT line cards and ONUs can be dynamically configured. The new OLT structure appears to be promising and cost-effective as compared to the WDM based solutions.

4.4 Optical Switch Specifications

Configuration time and power consumption of the optical switch are two main specifications that should be considered in the analysis.

4.4.1 Switch Configuration Time

Switches take time to change configurations. The switch reconfiguration time may affect the ONU performances when powering on/off OLT line cards. We investigate the impacts of the switch reconfiguration time on EPON and GPON, respectively.

- EPON: We argue that services of EPON ONUs are not affected when the switch configuration time is as large as 50 ms.

  In EPON, the upstream bandwidth allocation is controlled by OLT. ONUs transmit the upstream traffic using the allocated time durations stated in the GATE message. IEEE 802.3ah [5] specifies that ONUs need to send GATE messages every 50 ms to maintain registration even if they do not have traffic to transmit. Thus, the disrupted servicing time can be transparent to EPON ONUs when the switch reconfiguration time is as large as 50 ms, which can be satisfied by most optical switches.

- GPON: We argue that services of GPON ONUs are not affected when the switching time is no greater than $125\mu s$.

  For GPON, ITU-T G. 984.3 [4] specifies a fixed frame length of 125 μs. An ONU receives downstream control messages and sends its upstream data or control traffic every GPON frame, i.e., 125 μs. Therefore, services of GPON ONUs are not affected when the switch configuration time is no greater than $125\mu s$.

4.4.2 Power Consumption of Optical Switches

So far, we have not considered the impact of the power consumption of optical switches on the saved energy of OLT chassis. Optical switches consume some power, and the nonzero power consumption of optical switches may reduce the saved energy of the OLT chassis.

Denote $p(s)$ and $p(l)$ as the power consumption of the optical switch and one OLT line card, respectively. By incorporating the energy consumption of the optical switch, the power consumption of the proposed OLT chassis at any given time t equals to

$$p(l) \cdot l(t) + p(s) \tag{4.5}$$

Hence, the energy saving is reduced to

$$1 - \frac{p(l)/T \int_{t=0}^{T} l(t)dt + p(s)}{p(l) \cdot L} \tag{4.6}$$

The proposed OLT chassis can save some energy as compared to the legacy OLT chassis when the power consumption $p(s)$ of the optical switch satisfy the following condition

$$p(s) < (L - \frac{1}{T} \int_{t=0}^{T} l(t)dt) \cdot p(l) \tag{4.7}$$

The power consumption of optical switch differs from the switch size as well as the manufacturing technology. It is reported that one 2×2 optomechanic switch consumes around 0.2 w [3], while an OLT line card consumes around 5 w [48]. Then, for the $L = 2$ case, energy can be saved as long as the average number of power-on OLT line cards $\frac{1}{T}\int_{t=0}^{T} l(t)dt$ is less than 1.96. This condition can be easily satisfied. Therefore, even considering the power consumption of optical switches, the proposed OLT structure can still achieve a significant amount of power saving as compared to the legacy OLT.

4.5 System Model

In this section, Semi-Markov chains are employed to analyze the system. Different observation periods have been considered for decreasing and increasing the number of line cards. T_D is the observation time period for decreasing the number of active line cards. T_I is defined as an observation period for increasing the number of line cards. In order to ease the analysis, from now on, the formulations are based on the downstream traffic only. Poisson processes with the average rate of λ packets per second is assumed for downlink packet arrivals. The service time of each packet is assumed to be exponentially distributed with the average value of $1/\mu$. A fixed traffic scheduling cycle is assumed in the performance analysis. Consider $P_a(\alpha, T)$ and $P_d(\alpha, T)$ as the probability that α downstream packets arrive at the OLT chassis and depart from the OLT chassis during T traffic scheduling cycle, respectively:

$$P_a(\alpha, T) = e^{-\lambda T} \cdot \frac{(\lambda T)^{\alpha}}{\alpha!} \tag{4.8}$$

$$P_d(\alpha, T) = e^{-\mu T} \cdot \frac{(\mu T)^{\alpha}}{\alpha!} \tag{4.9}$$

The same process can be considered for uplink packet arrival in the case of having downstream and upstream traffic simultaneously.

4.5.1 OLT Chassis State

In the defined Markov chain model, the total number of active line cards vary from 1 to L. Therefore, there are L possible states of active line cards. A_i represents i active line cards. Transition from each active state to another active state should be done through the listening

states. There is no direct transition between active states. There are two different types of listening states: D (listening states for decreasing the number of line cards) and I (listening states for increasing the number of line cards). Figure 4.2 shows the state transitions.

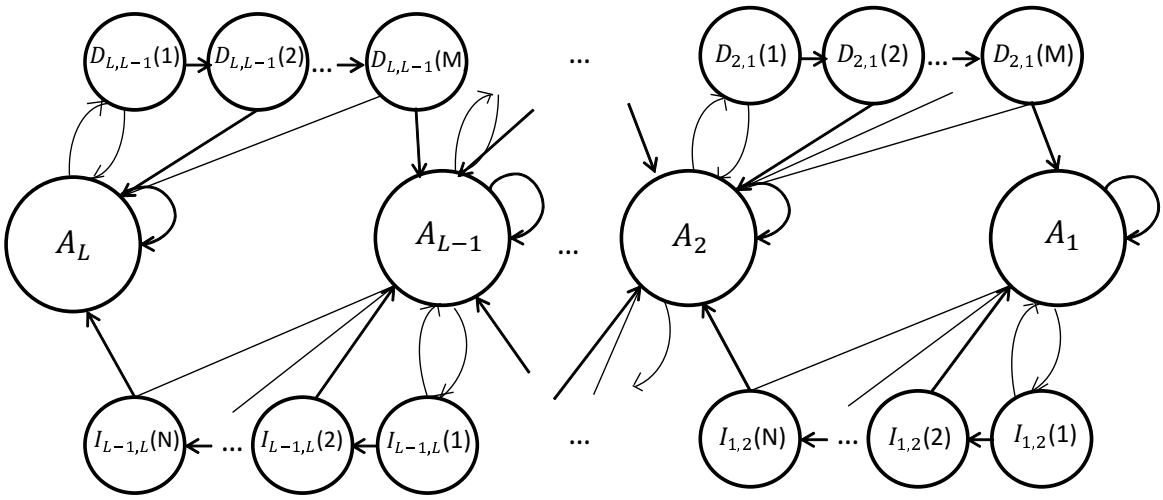

Figure 4.2 State transition in Markov chain.

$D_{i,i-1}(j)$ refers to the state that the total traffic load of the OLT chassis remains below i/L for j cycles. The number of active line cards during $M = T_D/T$ time cycles remains as i line cards. If the traffic load goes higher than i/L amount during a traffic scheduling cycle, the transition to A_i occurs. Otherwise, the transition from $D_{i,i-1}(j)$ to $D_{i,i-1}(j+1)$ happens. Whenever the number of listening cycles reaches M, the OLT chassis switches to the next lower active state (A_{i-1}).

$I_{i,i+1}(k)$ refers to the state that the total traffic load of the OLT chassis remains above i/L for k time cycles. The number of active line cards during $N = T_I/T$ remains as i line cards. The excess amount of the traffic will be buffered during T_I. If the traffic load becomes lower than i/L amount during a traffic scheduling cycle, the transition to A_i occurs. Otherwise, the transition from $I_{i,i+1}(k)$ to $I_{i,i+1}(k+1)$ happens. If the total traffic load stays beyond the defined threshold (i/L) for N traffic scheduling cycles, the OLT chassis switches to the next upper active state (A_{i+1}).

4.5.2 State Transitions

- State transitions from A_i to $D_{(i,i-1)}(1)$, $D_{(i,i-1)}(j)$ to $D_{(i,i-1)}(j+1)$, or from $D_{(i,i-1)}(M)$ to A_{i-1} for $i = 2, .., L$ and $j = 1, ..., M-1$ happen when the traffic load in a traffic scheduling cycle T is less than $(i-1)/L$. Therefore, by considering μ as the service rate of the OLT with $i-1$ active line cards, the probability that the number of arrival packets is smaller than the number of departure packets equals to: $\sum_{k=1}^{\infty}\sum_{j=0}^{\infty} P_a(j,T)P_d(j+k,T)$.

- State transitions from $I_{i,i+1}(k)$ to A_i for $i = 2, .., L$ and $k = 1, ..., N$ happen when the number of arrival packets in a traffic scheduling cycle T is smaller than or equal to the number of departure packets. μ in this case is the service rate of the OLT with i active line cards, and the probability equals to: $\sum_{k=0}^{\infty}\sum_{j=0}^{\infty} P_a(j,T)P_d(j+k,T)$.

- State transitions from A_i to $I_{(i,i+1)}(1)$, from $I_{(i,i+1)}(k)$ to $I_{(i,i+1)}(k+1)$, or from $I_{(i,i+1)}(N)$ to A_{i+1} for $i = 2, .., L$ and $k = 1, ..., N-1$ happen when the number of arrival packets in a traffic scheduling cycle T is greater than the number of departure packets. μ is the service rate of the OLT when i line cards are active. The probability equals to $\sum_{k=1}^{\infty}\sum_{j=0}^{\infty} P_a(j+k,T)P_d(j,T)$.

- State transitions from $D_{i,i-1}(j)$ to A_i for $i = 2, .., L$ and $j = 1, ..., M$ happen when the number of arrival packets in a traffic scheduling cycle T is greater than or equal to the number of departure packets. μ in this case is the OLT service rate with $i-1$ active line cards. The transition probability is $\sum_{k=0}^{\infty}\sum_{j=0}^{\infty} P_a(j+k,T)P_d(j,T)$.

- State transition from A_i to itself happens when the number of arrival packets in a traffic scheduling time T is greater than or equal to the number of departure packets with $i-1$ active line cards, and the number of arrival packets in a traffic scheduling cycle T is smaller than or equal to the number of departure packets with i active line cards. The probability is equal to $(\sum_{k=0}^{\infty}\sum_{j=0}^{\infty} P_a(j+k,T)P_d(j,T))(\sum_{k=0}^{\infty}\sum_{j=0}^{\infty} P_a(j,T)P_d(j+k,T))$.

4.5.3 Steady State Probabilities

Denote $P(A_i)$, $P(D_{i,i-1}(j))$ $(i = 2, ..., L\ j = 1, ..., M)$, and $P(I_{i,i+1}(k))$ $(i = 1, ..., L-1;$ $k = 1, ..., N)$ as the probability of the OLT state when the network is at its steady state. Therefore, the following constraints are satisfied. Steady state probabilities of all the active

states except $A(1)$ and $A(L)$ are as follows:

$$\begin{aligned}
&P(A_i)[pr\{A_i \rightarrow D_{i,i-1}(1)\} + pr\{A_i \rightarrow I_{i,i+1}(1)\}] \\
&= [\sum_{k=1}^{\infty} P(I_{i,i+1}(k)) pr\{I_{i,i+1}(k) \rightarrow A_i\}] \\
&+ P(I_{i-1,i}(N)) pr\{I_{i-1,i}(N) \rightarrow A_i\} \\
&+ \sum_{j=1}^{M} P(D_{i,i-1}(j)) pr\{D_{i,i-1}(j) \rightarrow A_i\} \\
&+ P(D-i+1, i(M)) pr\{D_{i+1,i}(M) \rightarrow A_i\} \\
&(i = 2, ..., L-1)
\end{aligned} \tag{4.10}$$

Steady state probability of A_1 is calculated as follows:

$$\begin{aligned}
&P(A_1) pr\{A_1 \rightarrow I_{1,2}(1)\} \\
&= \sum_{k=1}^{N} P(I_{1,2}(K) pr\{I_{1,2}(k) \rightarrow A_1\} \\
&+ P(D_{2,1}(M)) pr\{D_{2,1}(M) \rightarrow A_1\}
\end{aligned} \tag{4.11}$$

Steady state probability of A_L is acheived as follows:

$$\begin{aligned}
&P(A_L) pr A_L \rightarrow D_{L,L-1}(1) \\
&= \sum_{j=1}^{M} P(D_{L,L-1}(j)) pr\{D_{L,L-1}(j) \rightarrow A_L\} \\
&+ P(I_{L-1,L}(N)) pr\{P(I_{L-1,L}(N)) \rightarrow A_L\}
\end{aligned} \tag{4.12}$$

Steady state probability of listening states (D) except the first and last states are as follows:

$$\begin{aligned}
&P(D_{i,i-1}(j))[pr\{D_{i,i-1}(j) \rightarrow D_{i,i-1}(j+1)\} \\
&+ pr\{D_{i,i-1}(j) \rightarrow A_i\}] \\
&= P(D_{i,i-1}(j-1)) pr\{D_{i,i-1}(j-1) \rightarrow D_{i,i-1}(j)\} \\
&(i = 1, ..., L) \& (j = 2, ..., M-1)
\end{aligned} \tag{4.13}$$

Steady state probability of $D_{i,i-1}(1)$ equals to:

$$\begin{aligned} & P(D_{i,i-1}(1))[pr\{D_{i,i-1}(1) \rightarrow D_{i,i-1}(2)\} \\ & + pr\{D_{i,i-1}(1) \rightarrow A_i\}] \\ & = P(A_i) pr A_i \rightarrow D_{i,i-1}(1) (i = 1, ..., L) \end{aligned} \tag{4.14}$$

Steady state probability of $D_{i,i-1}(M)$ is as follows:

$$\begin{aligned} & D_{i,i-1}(M)[pr\{D_{i,i-1}(M) \rightarrow A_i\} \\ & + pr\{D_{i,i-1}(M) \rightarrow A_i - 1\}] \\ & = P(D_{i,i-1}(M-1)) pr\{D_{i,i-1}(M-1) \rightarrow D_{i,i-1}(M)\} \end{aligned} \tag{4.15}$$

The following is the steady state probability of the listening states I except the first and last states:

$$\begin{aligned} & p(I_{i,i+1}(k))[pr\{I_{i,i+1}(k) \rightarrow A_i\} + \\ & pr\{I_{i,i+1}(k) \rightarrow I_{i,i+1}(k+1)\}] \\ & = P(I_{i,i+1}(k-1)) pr\{I_{i,i+1}(k-1) \rightarrow I_{i,i+1}(k)\} \\ & (i = 1, ..., L) \& (k = 2, ...N-1) \end{aligned} \tag{4.16}$$

Steady state probability of $I_{i,i+1}(1)$ is as follows:

$$\begin{aligned} & P(I_{i,i+1}(1))[pr\{I_{i,i+1}(1) \rightarrow A_i\} \\ & + pr\{I_{i,i+1}(1) \rightarrow I_{i,i+1}(2)\}] \\ & = P(A_i) pr\{A_i \rightarrow Ii, i+1(1)\} (i = 1, ..., L) \end{aligned} \tag{4.17}$$

Steady state probability of $I_{i,i+1}(N)$ is obtained as follows:

$$\begin{aligned} & P(I_{i,i+1}(L))[pr\{I_{i,i+1}(L) \rightarrow A_i\} \\ & + pr\{I_{i,i+1}(L) \rightarrow A_{i+1}\}] \\ & = P(I_{i,i+1}(L-1)) pr\{I_{i,i+1}(L-1) \rightarrow Ii, i+1(L)\} \end{aligned} \tag{4.18}$$

Moreover, the sum of the probabilities of all the states is equal to 1, i.e.:

$$\sum_{i=1}^{L} P(A_i) + \sum_{i=1}^{L}\sum_{j=1}^{M} P(D_{i,i-1}(j)) + \sum_{i=1}^{L}\sum_{k=1}^{N} P(I_{i,i+1}(k)) = 1 \tag{4.19}$$

Therefore, the steady state probabilities of all the state can be calculated by solving the above equations 4.10-4.19.

4.5.4 Performance Analysis

Power Saving Denote $p(l)$ as the power consumption of one OLT line card and $P(A_i)$, $P(D_{i,i-1}(j))$ $(i = 2, ..., L\ j = 1, ..., M)$, and $P(I_{i,i+1}(k))$ $(i = 1, ..., L-1;\ k = 1, ..., N)$ as the probability of the OLT state when the network is at its steady state. Therefore, the average power consumption equals to:

$$p(l)[\sum_{i=1}^{L} ip(A_i) + \sum_{i=2}^{L}\sum_{j=1}^{M} ip(D_{i,i-1}(j)) + \sum_{i=1}^{L-1}\sum_{k=1}^{N} ip(I_{i,i+1}(k))] \tag{4.20}$$

4.5.5 Delay

Denote $E[\delta|\mathbb{A}_i]$, $E[\delta|\mathbb{D}_{i,i-1}]$, and $E[\delta|\mathbb{I}_{i,i+1}]$ as the conditional expectation of the delay for the packets which arrive when the OLT is in the states A_i, $D_{i,i-1}$, and $I_{i,i+1}$, respectively. Then, the average delay equals to

$$\sum_{i=1}^{L} E[\delta|\mathbb{A}_i]\cdot P(\mathbb{A}_i) + \sum_{i=2}^{L} E[\delta|\mathbb{D}_{i,i-1}]\cdot(\sum_{k=1}^{M} P(\mathbb{D}_{i,i-1}(k))) + \sum_{i=1}^{L-1} E[\delta|\mathbb{I}_{i,i+1}]\cdot(\sum_{k=1}^{N} P(\mathbb{I}_{i,i+1}(k))) \tag{4.21}$$

Considering the queuing delay, the average waiting time for these packets is:

$$E[\delta|\mathbb{A}_i] = \sum_{j=1}^{\infty}[p^a(j,T)(j-1)\cdot 1/(i\cdot\mu)] \tag{4.22}$$

$$E[\delta|\mathbb{D}_{i,i-1}] = \sum_{j=1}^{\infty}[p^a(j,T)(j-1)\cdot 1/(i\cdot\mu)] \tag{4.23}$$

$$E[\delta|\mathbb{I}_{i,i+1}] = \sum_{j=1}^{\infty}[p^a(j,T)(j-1)\cdot 1/(i\cdot\mu)] \tag{4.24}$$

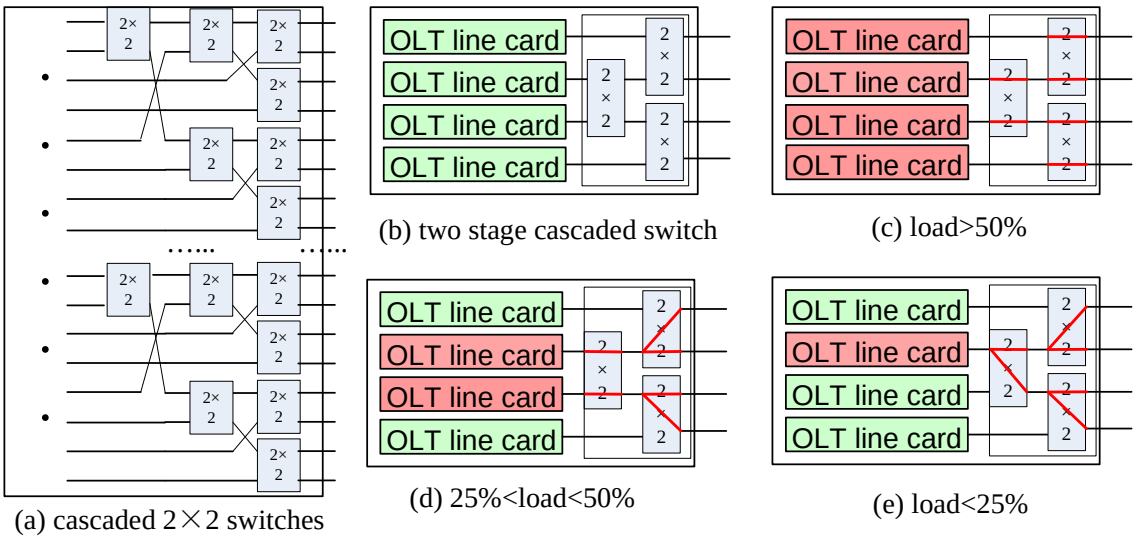

Figure 4.3 OLT with multi-stage cascaded switches.

4.6 Cost Reduction

Another problem with optical switches is their high prices. The prices of optical switches vary from their manufacturing techniques [39]. At present, there are generally four kinds of optical switches: opto-mechanical switches, micro-electro-mechanical system (MEMS), electro-optic switches, and semiconductor optical amplifier switches. Currently, the opto-mechanic switches are less expensive than the other three kinds. Simply because of their low prices, opto-mechanic switches are generally the adopted choice in designing energy-efficient OLT.

4.6.1 OLT with Cascaded 2×2 Switches

For opto-mechanic switches, an important constraint is their limited port counts. Popular sizes of opto-mechanic switches are 1×2 and 2×2. Considering the port count constraints, we further propose the cascaded 2×2 switches structure to achieve the dynamic configuration of OLT. More specifically, to replace an $N \times N$ switch, the cascaded 2×2 switch contains $\log_2^N$ stages and $(N-1)$ 2×2 switches. Figure 4.3(a) illustrates the proposed cascaded switches. In the switch, the kth stage contains $2^{(k-1)}$ switches.

Figure 4.3(b) shows a two-stage cascaded 2×2 switches to replace a 4×4 switch. As illustrated in Figure 4.3(c)-(e), when the traffic load is greater than 50%, one PON system is connected with one OLT line card; when the traffic load is between 25% and 50%, two

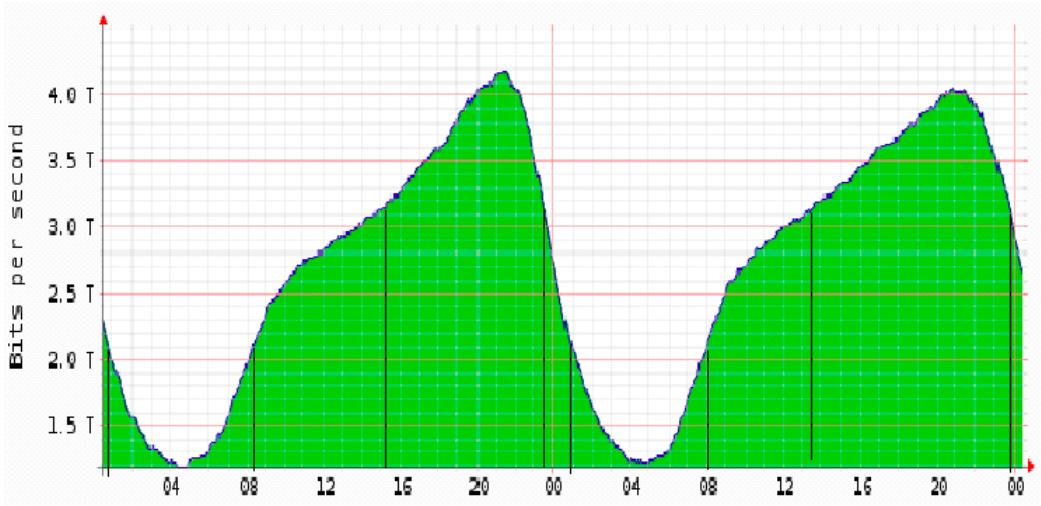

Figure 4.4 Daily traffic profile.
source:[6].

PON systems are connected with one OLT line card; when the traffic load is less than 25%, all PON sytems are connected with a single OLT line card.

4.6.2 Analysis

Here, we analyze the saved energy of the proposed OLT equipped with cascaded switches. Assume the traffic is uniform among all ONUs. Then, when the traffic load is between 50% and 100%, all OLT line cards need be power-on; when the traffic load is between 25% and 50%, half of the OLT line cards are powered on.

To explore the efficiency of the proposed OLT structure, we calculate the saved energy in the following example. Figure 4.4 shows the typical daily profile of aggregated traffic on all Amsterdam Internet Exchange member ports on Feb. 25 and Feb. 26, 2016 [6]. During the time period of 48 hours, the time durations that the network remains in each traffic load interval are listed as follows:

- $load < 25\% : 0$
- $25\% < load < 50\% : (8.5 - 1) + (8 - 1) = 14.5$
- $50\% < load < 75\% : (1-0)+(14.5-8.5)+(24-23.5)+(1-0)+(13.5-8)+(24-23.5) = 14.5$
- $load > 75\% : (23.5 - 14.5) + (23.5 - 13.5) = 19$

Note that the energy saving of the OLT chassis is related to the number of OLT line cards and the number of connecting ONUs. Owing to the rounding effect, the energy saving increases with the increase of the number of OLT line cards.

Considering an OLT chassis with 4 OLT line cards equipped with a 4×4 switch, energy saving equals to:

$$1 - (14.5 * 2 + 14.5 * 3 + 19 * 4)/4 * 48 = 22.65\%$$

When the OLT is equipped with cascaded 2×2 switches, the energy saving equals to:

$$1 - (14.5 * 2 + 33.5 * 4)/4 * 48 = 15.1\%$$

For the two-stage cascaded switch, the relative energy saving is 15.1%, which is slightly smaller than the 4×4 switch case. Since traffic of a much smaller number of users is aggregated, a larger burstiness should be observed for the traffic arriving at the central office as compared to that shown in Figure 4.4. Hence, a higher saving will be achieved than the saving shown in this example.

Generally, when the traffic load is between $1/2^k$ and $1/2^{k+1}$, $1/2^k$ of the OLT line cards are power-on. Therefore,

$$\begin{aligned} 1/2^{k+1} \leq load \leq 1/2^k \\ k = \lfloor \log_2 (1/load) \rfloor \\ l(t) = 1/2^{\lfloor \log_2 (1/load) \rfloor} \end{aligned} \tag{4.25}$$

The saved energy equals to

$$1 - 1/2^{\lfloor \log_2 (1/load) \rfloor} \tag{4.26}$$

As compared to the OLT with an $N \times N$ switch, the OLT with cascaded 2×2 switches saves a less amount of energy.

Note that the typical switching speed of the opto-mechanical switch is around 5 ms. As discussed before, it does not affect the performances of users in EPON, but may have impacts on the performances of users in GPON.

4.7 OLT with Electrical Switches

Another scheme of avoiding the significant cost increase is to use electrical switches instead. However, before aggregating traffic using electrical switches, the optical transceivers are required to convert the optical signals into electrical signals. Thus, only the energy consumption of the electrical part in an OLT line card can be saved. The energy saving is limited as compared to the scheme of using optical switches. Let $p(e)$ be the energy consumption of the electrical part of an OLT line card. Then, the average energy saving of the OLT equipped with an electrical switch equals to:

$$1 - \frac{l(t) \cdot p(e)}{L \cdot p(l)} \tag{4.27}$$

The efficiency of energy saving of this scheme depends on the ratio $p(e)/p(l)$.

4.8 Performance Evaluation

In this section, the performance of the sleep control scheme of the OLT line cards for Poisson and non-Poison traffic is studied using simulations. For the theoretical analysis, Poisson process for the packet arrival and exponential distribution for the packet service time is considered as they are theoretically tractable.

The numerical results are based on the analysis in Section 4.5. Since self-similarity is exhibited in many applications, and the actual network traffic with bursts is self-similar, our simulation is also conducted for self-similar traffic with the Hurst parameter of 0.8. The packet length is uniformly distributed between 64 bytes and 1518 bytes. To show the accuracy of the work, we compare the simulation results with the numerical results of the Markov model. In the figures, "Poisson (num)" represents the numerical results for Poisson traffic, "Poisson (sim)" shows the simulation results for Poisson traffic, and "Self-similar (sim)" indicates the simulation results for self-similar traffic.

The total number of line cards is assumed to be 4 with the capacity of $1Gb/s$ for each line card. The time duration of each traffic scheduling cycle is considered to be $2ms$.

Energy saving in the simulation results is normalized. This shows a comparison between our proposed scheme and the base model in which no sleep scheme is defined. In Figure 4.5, the numerical results of the Markov model and the simulation results for the energy

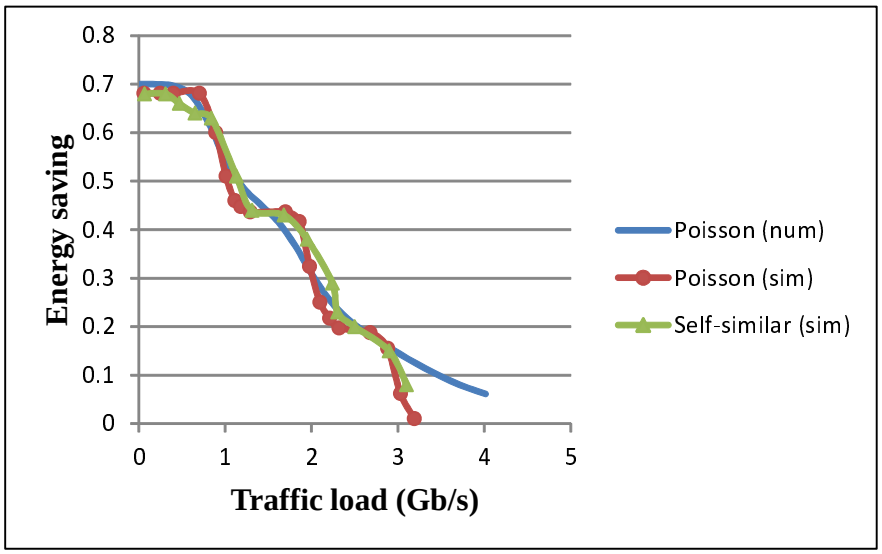

Figure 4.5 Energy saving vs. arrival traffic rate.

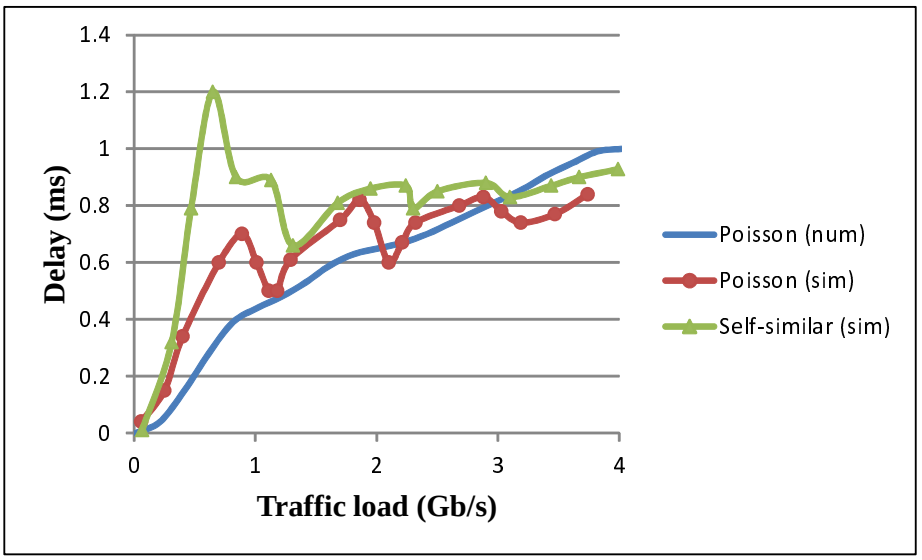

Figure 4.6 Delay vs. arrival traffic rate.

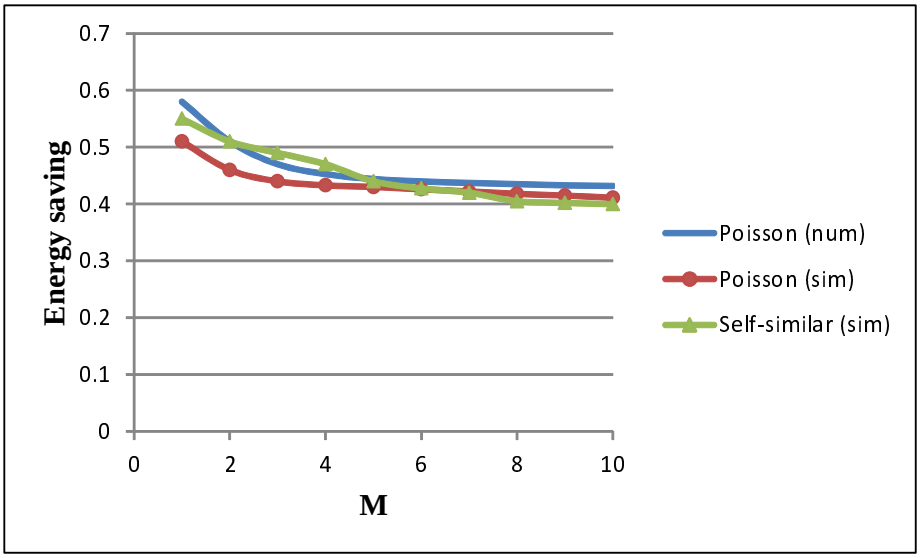

Figure 4.7 Energy saving vs. M listen cycles.

saving performance under different traffic arrival rates are illustrated. It is assumed that the maximum number of "D" listen cycles (M) as well as the maximum number of "I" listen cycles (N) equal to 2. The arrival traffic is increased up to $4Gb/s$. As the arrival traffic increases, the energy saving decreases as the OLT chassis needs to power on more active line cards to support the arrival traffic. When the arrival traffic is less than $1Gb/s$, one line card is sufficient to satisfy the traffic and the other 3 line cards are shut down. Therefore, the maximum energy saving is achieved.

Figure 4.6 shows delay performance under different traffic arrival rate. With the increase of the traffic rate, the queuing delay increases, and thus the average delay increases. As more line cards are activated, service rate increases and delay decreases. Obviously, by increasing traffic arrival rate, With the fixed number of active line cards, queuing delay decreases.

As it can be seen in Figure 4.5 and Figure 4.6, the numerical results match the simulation results for Poisson traffic, and the trend of energy saving and delay performance by increasing the traffic load for self-similar traffic is also similar to that of the Markov model for Poisson traffic. Therefore, the applicability of the proposed scheme on real-time traffic is confirmed.

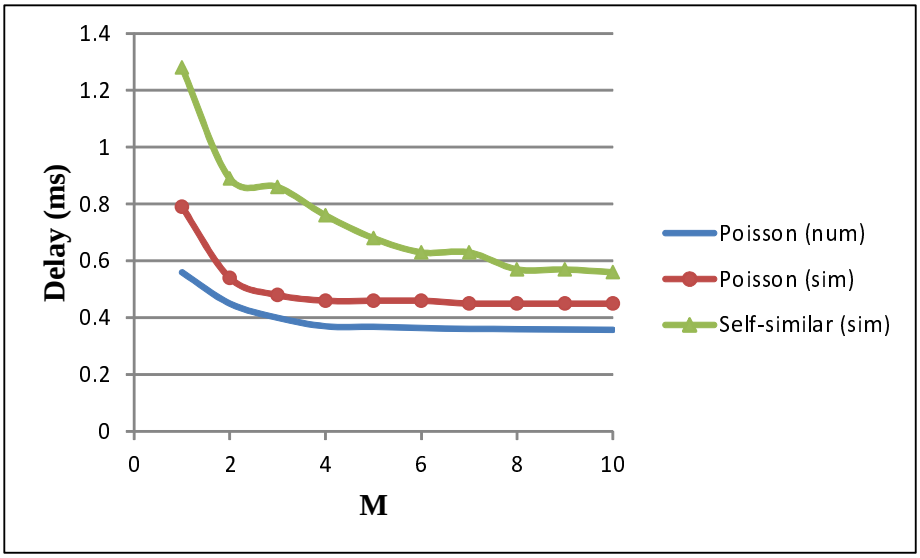

Figure 4.8 Delay vs. M listen cycles.

Before decreasing the number of OLT line cards, the OLT chassis needs to monitor the traffic for the maximum of M listen cycles. Figure 4.7 shows the effect of changing the number of M on energy saving for Poisson and self-similar traffic. The average arrival traffic is set to $1.11Gb/s$, and the number of N listen cycle is set to 2. With the increase of M, the OLT chassis needs to keep a larger number of line cards active for the time duration of $M \cdot T$. Thus, the energy saving decreases by increasing M.

Figure 4.8 shows the impact of different M listen cycles on the delay performance. During M cycles, the number of active line cards is more than necessary. Therefore, the packets encounter less delay, and delay decreases with the increase of M. Similar to the theoretical analysis of Poisson traffic, energy saving and delay decrease as the number of listen cycles increases for both Poisson and self-similar traffic.

N is the maximum number of traffic cycles during which the OLT chassis needs to monitor the traffic before increasing the number of line cards. With the increase of N, the energy saving increases as the number of active line cards is smaller for the total duration of $N \cdot T$. Essentially, as illustrated in Figure 4.9, increasing the N cycles helps saving more energy in both Poisson and self-similar traffic. In this simulation, the average arrival traffic is set to $1.98Gb/s$, and the number of M listen cycle is set to 2.

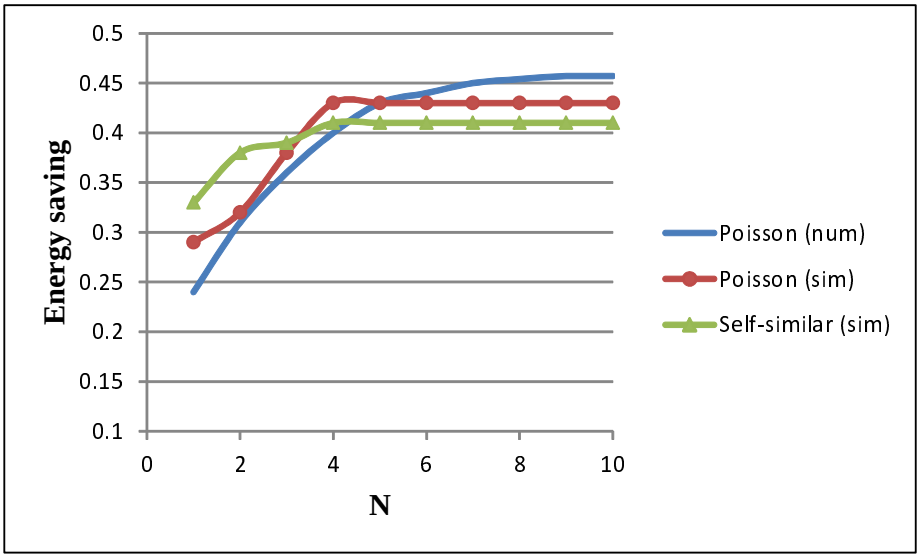

Figure 4.9 Energy saving vs. N listen cycles.

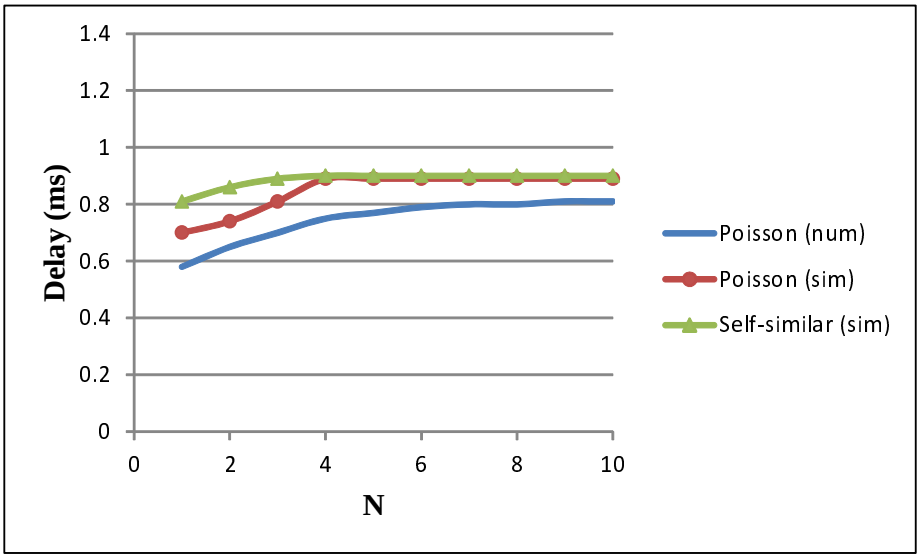

Figure 4.10 Delay vs. N listen cycles.

As mentioned earlier, during "I" listen cycles, the OLT chassis receives traffic load more than the available line cards. Before increasing the number of line cards, the OLT chassis needs to monitor the traffic for N cycles. During theses cycles, the number of line cards stay the same, and the OLT buffers the extra traffic. The buffered packets encounter some delay as depicted in Figure 4.10. Therefore, proper setting of N needs to be considered to save energy without impairing the QoS of the users.

4.9 Summary

A novel energy-efficient OLT structure has been proposed in this chapter to adapt its power-on line cards to the real-time arrival traffic. Specifically, we have added a switch into the legacy OLT chassis to dynamically configure the connection between OLT line cards and ONUs. We first describe an OLT equipped with an $N \times N$ switch, and investigate the impacts of the power consumption of the optical switch and switch configuration time on the saved energy of the whole OLT chassis. Then, to avoid a dramatic cost increase, we advocate the use of opto-mechanical switches among all currently commercially-available switches, and further propose to use a cascaded 2×2 switch structure. To decrease the frequent change of status of the line cards, a sleep mechanism has been proposed. By employing semi-markov chain, the performance of the proposed scheme is analyzed. The analysis demonstrates that the proposed OLT achieves significant power savings as compared to the legacy OLT.

CHAPTER 5

CONCLUSION

Ethernet Passive Optical Networks (EPONs) are considered as one of the most attractive architectures for FTTx deployment. Enabling sleep mode for the ONUs is currently the most promising solution to reduce power consumption in ONUs and consequently PON. In this dissertation, the challenges of reducing the energy consumption of optical elements have been discussed. In Chapter 2, a novel solution has been proposed based on the mutual inference between the ONU and the OLT. The proposed scheme is compatible with the IEEE802.3ah standards and no modification is needed in the MAC control protocol. The performance of the proposed algorithm is demonstrated through the numerical and simulation results. Since the ONU can disable some performing functions, different level of ONU power consumption has been defined in Chapter 3. The ONU transmitter and the receiver can separately go to the sleep mode based on the upstream and downstream traffic situations. Moreover, an analytic model is proposed to compute the maximum sleep time of the ONU transmitter based on the maximum delay requirement of each class of service. Numerical and simulation results have been conducted to prove the correctness of the presented model. In PONs, energy is consumed by both optical line terminal (OLT) and optical network unit (ONU). Owing to the large quantity, ONUs consume a large portion of the overall PON energy. Although OLT consumes a less amount of power than the total aggregated ONUs, one OLT line card does consume a much larger amount of power than that of one ONU. Reducing energy consumption of OLT is as important as reducing energy consumption of ONUs especially from the operators and home users perspectives. For the network operators, decreasing the energy consumption of OLT can significantly reduce the energy consumption of the central office, while decreasing the energy consumption of ONUs has small and likely negligible impacts on that of home users who have many other electrical appliances with much higher energy consumption. Since the actual network traffic is usually less than the provided capacity, potentially low energy consumption can be achieved. In Chapter 4, a green OLT which can provide variable data rates has been designed to properly vary PON rates without degrading

service quality. In order to analyze the system, we have employed semi-Markov chains and derived a closed form expression for the average power consumption of the OLT chassis.

5.1 Future Challenges to Overcome

According to Energy 2020, access network power supplies and edge facilities consume over 70% of a cable operator's energy consumption. Therefore, substantial innovation is needed to further enhance energy efficiency in these areas, i.e., edges that house headend and hub equipment, especially OLT. While a solution to reduce energy consumption of OLT has been proposed, fixed-rate OLT line cards limit further energy saving. To satisfy the QoS requirements, when the traffic load is slightly higher than the capacity of a line card, the second line card needs to be activated. Digital signal processing can be utilized to build rate adaptive transceivers. Such software-defined transceivers can support a set of data rates without increasing the number of wavelength channels. Therefore, the OLT can update the wavelength data rate based on the traffic volume in a finer granularity and can thus potentially achieve further energy saving. Designing such capacity-adaptive optical transceivers remains a challenging issue.

Immediately after XG-PON1 has been standardized, FSAN began to work on NG-PON2 to increase the bandwidth beyong 10 Gbit/s. In 2012, time- and wavelength-division multiplexed passive optical network (TWDM-PON) was selected as the primary solution to NG-PON2 [40, 38]. In TWDM architecture, multiple XG-PONs are stacked using WDM to increase the aggregate PON rate. The proposed ONU energy saving scheme for TDM PON can still be applied to TWDM PON for the ONUs of the same wavelength. However, presence of multiple transmitters and receivers at the OLT poses several challenges for improving the OLT energy saving.

BIBLIOGRAPHY

[1] ITU-T recommendation G. 114: One-way transmission time. `http://www.itu.int/rec/T-REC-G/e` (accessed on April 20 2016), 2000.

[2] ITU-T recommendation G. 1010: End-user multimedia QoS categories (quality of service and performance). `http://www.itu.int/rec/T-REC-G/e` (accessed on April 20 2016), 2001.

[3] 2x2 opto-mechanical switch. `http://www.unitedoptronics.com/Datasheet/OpticalSwitch/OSW_2x2.pdf` (accessed on April 20, 2016), 2008.

[4] ITU-T recommendation G. 984 series. `http://www.itu.int/rec/T-REC-G/e` (accessed on April 20 2016), 2008.

[5] *IEEE draft standard for information technology–telecommunications and information exchange between systems–local and metropolitan area networks–specific requirements part 3: carrier sense multiple access with collision detection (CSMA/CD) access method and physical layer specifications amendment: physical layer specifications and management parameters for 10 Gb/s passive optical networks.* IEEE approved Draft Std P802.3av/D3.4, IEEE, Piscataway, NJ, 2009.

[6] Aggregated traffic on all ams-ix connected networks ports. `https://ams-ix.net/technical/statistics` (accessed on April 20, 2016), 2016.

[7] N. Ansari and J. Zhang. *Media Access Control and Resource Allocation for Next Generation Passive Optical Networks.* New york, NY: Springer, 2013.

[8] C. M Assi, Y. Ye, S. Dixit, and M. Ali. Dynamic bandwidth allocation for quality-of-service over ethernet PONs. *IEEE Journal on Selected Areas in Communications*, 21(9):1467–1477, 2003.

[9] J. Baliqa, R. Avre, K. Hinton, W. V. Sorin, and R. S. Tucker. Energy consumption in optical IP networks. *IEEE/OSA Journal of Lightwave Technology*, 27(13):2391–2403, 2009.

[10] J. Baliqa, R. Avre, W. V. Sorin, K. Hinton, and R. S. Tucker. Energy consumption in access networks. In *Optical Fiber Communication (OFC) Conference*, 2008.

[11] A. Banerjee, Y. Park, F. Clarke, H. Song, S. Yang, G. Kramer, K. Kim, and B. Mukherjee. Wavelength-division-multiplexed passive optical network (WDM-PON) technologies for broadband access: a review [invited]. *Journal of Optical Networking*, 4(11):737–758, 2005.

[12] D. P. Bertsekas, R. G. Gallager, and P. Humblet. *Data Networks*, volume 2. Upper Saddle River, NJ: Prentice-Hall International, 1992.

[13] P. Brooks and B. Hestnes. User measures of quality of experience: why being objective and quantitative is important. *IEEE Network*, 24(2):8–13, 2010.

[14] H.-L. Chao and W. Liao. Credit-based slot allocation for multimedia mobile ad hoc networks. *IEEE Journal on Selected Areas in Communications*, 21(10):1642–1651, 2003.

[15] P. Chowdhury, M. Tornatore, and B. Mukherjee. On the energy efficiency of mixed-line-rate networks. In *National Fiber Optic Engineers Conference*, pages 1–3, 2010.

[16] K. J. Christensen, B. Gunaratne, and A. D. George. The next frontier for communications networks: power management. *Computer Communications*, 27(18):1758–1770, 2004.

[17] A. R. Dhaini, P.-H. Ho, G. Shen, and B. Shihada. Energy efficiency in TDMA-based next-generation passive optical access networks. *IEEE/ACM Transactions on Networking (TON)*, 22(3):850–863, 2014.

[18] M. Ergen. *Mobile broadband: including WiMAX and LTE*. Springer Science & Business Media, 2009.

[19] G. Fettweis and E. Zimmermann. Ict energy consumption-trends and challenges. volume 2. IEEE, 2008.

[20] M. Gupta and S. Singh. Using low-power modes for energy conservation in Ethernet LANs. In *26th IEE Int'l Conf. on Computer Communications (INFOCOM2007)*, pages 2451–2455, 2007.

[21] L. Hutcheson. Fttx: Current status and the future. *IEEE Communications Magazine*, 46(7):90–95, 2008.

[22] J. Kani, S. Shimazu, N. Yoshimoto, and H. Hadama. Energy-efficient optical access networks: issues and technologies. *IEEE Communications Magazine*, 51(2):S22–S26, 2013.

[23] K. S. Kim. On the evolution of PON-based FTTH solutions. *Information Sciences*, 149(1):21–30, 2003.

[24] G. Kramer. Self-similar network traffic. `http://glenkramer.com/trf_research.shtml` (accessed on April 20, 2016), 2001.

[25] G. Kramer. *Ethernet passive optical networks*. New york, NY: McGraw-Hill, 2005.

[26] G. Kramer, M. De Andrade, R. Roy, and P. Chowdhury. Evolution of optical access networks: Architectures and capacity upgrades. *Proceedings of the IEEE*, 100(5):1188–1196, 2012.

[27] G. Kramer, B. Mukherjee, S. Dixit, Y. Ye, and R. Hirth. Supporting differentiated classes of service in ethernet passive optical networks. *Journal of Optical Networking*, 1(9):280–298, 2002.

[28] G. Kramer and G. Pesavento. Ethernet passive optical network (epon): building a next-generation optical access network. *IEEE Communications magazine*, 40(2):66–73, 2002.

[29] R. Kubo, J. Kani, H. Ujikawa, T. Sakamoto, Y. Fujimoto, N. Yoshimoto, and H. Hadama. Study and demonstration of sleep and adaptive link rate control mechanism for energy efficient 1G-EPON. *IEEE/OSA Journal of Optical Communications and Networking*, 2(9):716–729, 2010.

[30] C. Labovitz, S. Iekel-Johnson, D. McPherson, J. Oberheide, and F. Jahanian. Internet inter-domain traffic. *ACM SIGCOMM Computer Communication Review*, 41(4):75–86, 2011.

[31] C. Lange, M. Braune, and N. Gieschen. On the energy consumption of FTTB and FTTH access networks. In *National Fiber Optic Engineers Conference*, 2008.

[32] C. Lee, W. V. Sorin, and B. Kim. Fiber to the home using a PON infrastructure. *IEEE/OSA Journal of Lightwave Technology*, 24(12):4568–4583, 2006.

[33] S. Lee and A. Chen. Design and analysis of a novel energy efficient ethernet passive optical network. In *Ninth International Conferenece on Networks (ICN)*, pages 6–9, 2010.

[34] M. Li. Self-similarity and long-range dependence in teletraffic. In *the 9th WSEAS International Conference on Multimedia Systems & Signal Processing*, pages 19–24, 2009.

[35] B Lung. PON architecture futureproofs ftth. *Lightwave, PennWell*, 16(10):104–107, 1999.

[36] Y. Luo and N. Ansari. Bandwidth allocation for multiservice access on EPONs. *IEEE Communications Magazine*, 43(2):S16–S21, 2005.

[37] Y. Luo, S. Yin, N. Ansari, and T. Wang. Resource management for broadband access over TDM PONs. *IEEE Network*, 21(5):20–27, 2007.

[38] Y. Luo, X. Zhou, F. Effenberger, X. Yan, G. Peng, Y. Qian, and Y. Ma. Time- and wavelength-division multiplexed passive optical network (twdm-pon) for next-generation PON stage 2 (ng-pon2). *Journal of Lightwave Technology*, 31(4):587–593, 2013.

[39] X. Ma and G. Kuo. Optical switching technology comparison: optical mems vs. other technologies. *IEEE Communications Magazine*, 41(11):16–23, 2003.

[40] Y. Ma, Y. Qian, G. Peng, X. Zhou, X. Wang, J. Yu, Y. Luo, X. Yan, and F. Effenberger. Demonstration of a 40gb/s time and wavelength division multiplexed passive optical network prototype system. In *Optical Fiber Communication Conference*, pages PDP5D–7. Optical Society of America, 2012.

[41] J. Mandin. EPON power saving via sleep mode. In *IEEE P802. 3av 10GEPON Task Force Meeting*, 2008.

[42] M. Pickavet, W. Vereecken, S. Demever, P. Audenaert, B. Vermeulen, C. Develder, D. Colle, B. Dhoedt, and P. Demeester. Worldwide energy needs for ict: the rise of power-aware networking. In *2nd International Symposium on Advanced Networks and Telecommunication Systems*, pages 1–3. IEEE, 2008.

[43] K. Qiu, X. Yi, L. Zhang, H. Zhang, M. Deng, and C. Zhang. OFDM-PON optical fiber access technologies. In *Communications and Photonics Conference and Exhibition, 2011. ACP. Asia*, pages 1–9. IEEE, 2011.

[44] R. Q. Shaddad, M. Abu Bakar, S. M. Idrus, A. M. Al-hetar, and N. A. Al-geelani. Emerging optical broadband access networks from TDM PON to OFDM PON. *PIERS Proceedings*, 3:4, 2012.

[45] M. Taheri and N. Ansari. Multi-power-level energy saving management for passive optical networks. *IEEE/OSA Journal of Optical Communications and Networking*, 6(11):965–973, 2014.

[46] K. Tanaka. 10G-EPON standardization and its development status. In *National Fiber Optic Engineers Conference*, page NThC4. Optical Society of America, 2009.

[47] R. W. Tkach. Network traffic and system capacity: Scaling for the future. In *36th European Conference on Optical Communication (ECOC)*, pages 1–22. IEEE, 2010.

[48] W. Vereecken, Ward V. Heddeghem, M. Deruvck, P. Bart, L. Bart, J. Wout, and P. Demeester. Power consumption in telecommunication networks: overview and reduction strategies. *IEEE Communications Magazine*, 49(6):62–69, 2011.

[49] E. Wong, M. Mueller, M. PI Dias, Chien A. C., and M. Amann. Energy-efficiency of optical network units with vertical-cavity surface-emitting lasers. *Optics Express*, 20(14):14960–14970, 2012.

[50] S. Wong, S. Yen, P. Afshar, S. Yamashita, and L. Kazovsky. Demonstration of energy conserving TDM-PON with sleep mode ONU using fast clock recovery circuit. In *Optical Fiber Communication Conference*, 2010.

[51] S.W. Wong, L. Valcarenghi, S.H. Yen, D.R Campelo, S. Yamashita, and L.G. Kazovsky. Sleep mode for energy saving PONs: Advantages and drawbacks. In *IEEE GLOBECOM Workshops09*, pages 1–6, 2009.

[52] Y. Xiao, X. Du, and J. Zhang. Internet protocol television (iptv): the killer application for the next-generation internet. In *Institute of Electrical and Electronics Engineers*, 2007.

[53] Y. Yan and L. Dittman. Energy efficiency in Ethernet Passive Optical Networks (EPONs): Protocol design and performance evaluation. *Journal of Communication*, 6(3):249–261, 2011.

[54] Y. Yan, S. Wong, L. Valcarenghi, S. Yen, D. Campelo, S. Yamashita, Kazovsky L., and Dittmann L. Energy managment mechanism for Ethernet Passive Optical Networks (EPONs). In *IEEE International Conference on Communications (ICC)*, 2010.

[55] J. Zhang and N. Ansari. An application-oriented resource allocation scheme for EPON. *IEEE Systems Journal*, 4(4):424–431, 2010.

[56] J. Zhang and N. Ansari. Dynamic time allocation and wavelength assignment in next-generation multi-rate multi-wavelength passive optical networks. In *IEEE International Conference on Communications (ICC)*, pages 1–5, 2010.

[57] J. Zhang and N. Ansari. Toward energy-efficient 1G-EPON and 10G-EPON with sleep-aware mac control and scheduling. *IEEE Communications Magazine*, 49(2):S33–S38, 2011.

[58] J. Zhang, N. Ansari, Y. Luo, F. Effenberqer, and F. Ye. Next-generation PONs: a performance investigation of candidate architectures for next-generation access stage 1. *IEEE Communications Magazine*, 47(8):49–57, 2009.

[59] J. Zhang, M. Taheri Hosseinabadi, and N. Ansari. Standards-compliant EPON sleep control for energy efficiency: Design and analysis. *IEEE/OSA Journal of Optical Communications and Networking*, 5(7):677–685, 2013.

[60] J. Zhang, T. Wang, and N. Ansari. Designing energy-efficient optical line terminal for TDM passive optical networks. In *34th IEEE Sarnoff Symposium*, 2011.

[61] Y. Zhang, P. Chowdhury, M. Tornatore, and B. Mukherjee. Energy efficiency in telecom optical networks. *IEEE Communications Surveys & Tutorials*, 12(4):441–458, 2010.

[62] J. Zheng and H. T Mouftah. Media access control for ethernet passive optical networks: an overview. *IEEE Communications Magazine*, 43(2):145–150, 2005.